Few-Body Systems 39, 123–157 (2006)
DOI 10.1007/s00601-006-0161-3

Few-Body Systems
Printed in Austria

Solution of the Spectator Equation for Relativistic *NN* Scattering Without Partial Wave Expansion

G. Ramalho[1,2,*], A. Arriaga[2,3,**], and M. T. Peña[1,4,***]

[1] Centro de Física Teórica das Partículas, Av. Rovisco Pais 1, 1049-001 Lisboa, Portugal
[2] Centro de Física Nuclear da Universidade de Lisboa, Av. Prof. Gama Pinto 2, 1649-003 Lisboa, Portugal
[3] Departamento de Física, Faculdade de Ciências da Universidade de Lisboa, 1700 Lisboa, Portugal
[4] Departamento de Física, Instituto Superior Técnico, Av. Rovisco Pais 1, 1049-001 Lisboa, Portugal

Received January 24, 2006; accepted May 26, 2006
Published online August 30, 2006;

Abstract. We developed a numerical method, based on the Padé summation, to solve the covariant spectator equation without partial wave decomposition, and applied it to the *NN* system. We present a general analytical formula for the polar angle integration, and a new prescription to handle the singularities present in the kernel of the spectator equation, due to the anti-symmetrization condition. The convergence of the partial wave-decomposition series is tested as a function of the energy. The on- and off-mass-shell amplitudes are calculated. The *NN* model was fitted to the *np* differential cross section, up to 320 MeV laboratory energy.

1 Introduction

For reliable information to be extracted from momentum transfer processes in the few GeV/c region, such as electron scattering off light nuclei [1, 2], a description based on relativistic kinematics and dynamics is required. On the other hand, traditional numerical methods to solve dynamical equations are based upon partial wave decomposition (PWD) of the *NN* interaction, but above 300 MeV the con-

* *E-mail address*: gilberto.ramalho@cftp.ist.utl.pt
** *E-mail address*: arriaga@cii.fc.ul.pt
*** *E-mail address*: teresa@cftp.ist.utl.pt

vergence of the series for the transition scattering amplitudes requires partial waves corresponding to total angular momentum up to $J = 15$ [3]. This makes the method not practical when those amplitudes at high energies are needed as input for calculations of three nucleons [4], or more complex particle systems.

Since for the energy range mentioned relativity becomes an issue, in this work we develop, and test, a method to solve relativistic quasi-potential equations, or the *NN* system, without PWD, in particular the spectator equation [5, 6] with a realistic *NN* interaction. The present paper prepares for later applications to photo- and electro-reactions at high energies.

The results of the work presented here indicate that methods not based on PWD generate numerical equations which (i) present much less analytical and algebraic complexity than alternative formulations with PWD, (ii) are appropriate for the energy region where PWD converges too slowly, and which is probed by the Jefferson Lab (Jlab) data for electro- and photo-disintegration of the two- and three-nucleon systems, (iii) although technically complex, are solvable within reasonable CPU time by present-day computer resources, whose limitations are not any more a serious objection to directly solve three-dimensional integral equations.

The spectator quasi-potential equation incorporates relativistic effects such as retardation and negative-energy state components. The focus here is on obtaining a working method to solve that equation without PWD, proceeding directly through a three-dimensional integration.

The numerical size of the relativistic problem is twice as large as the one of the non-relativistic case. The resulting equation couples 8 channels corresponding to the different final helicities and the $(+,-)$ energy-propagator components. To reduce computing time, we performed the polar-angle integration analytically. Another new feature of the method presented here is the way it deals with the singularities from the exchange kernel, demanded by the anti-symmetrization requirement. This is the first work that combines the two aspects, relativity and three-dimensional numerical methods, in an application to the scattering problem of two-nucleon systems.

In Sect. 2 an overview of three-dimensional methods and of quasi-potential equations and, in particular, the spectator equation for fermions is presented. In Sect. 3 the method of solving the integral equation without partial wave decomposition is explained in detail. In Sect. 4 results for *NN* on-mass-shell amplitudes, the *NN* differential cross section, and *NN* off-mass-shell amplitudes are shown and discussed. Finally, Sect. 5 presents the conclusions.

2 Background

2.1 Three-Dimensional (3D) Methods

For energies not larger than 300 MeV, numerical methods without partial wave decomposition, also referred to as three-dimensional (3D) methods [3], were applied to non-relativistic *NN* scattering using the Bonn and Argonne interactions.

In applications to the three-nucleon system presented in ref. [4] the PWD method was realized to be inappropriate for three-nucleon processes at energies higher than 250 MeV. At these energies, both two- and three-nucleon scattering amplitudes were seen to exhibit a strong angular dependence in the forward and backward scattering

angles, preventing an efficient and reasonable description in terms of a few partial waves. Other non-relativistic calculations without partial wave decomposition for the amplitudes of the two- and three-scalar particle systems were published [7, 8]. Within the relativistic approaches, ref. [9] compares different quasi-potential equations for scalar particles and interactions, using 3D methods. As pointed out by refs. [8], the dependence of the widely used one-boson-exchange (OBE) potentials on momentum vectors can be rather simple in the 3D methods, whereas the partial wave representation of those potentials involves rather complicated expressions.

2.2 Quasi-Potential (QP) Equations

When dealing with the *NN* system, a usual approximation of the Bethe-Salpeter equation [10] consists of restricting the integral kernel to a sum of OBE diagrams, which is often called the ladder approximation. Nevertheless, this approximation may be questioned. In fact, the one-body limit is not recovered when one of the particle masses goes to infinity [5, 11]. Moreover, the crossed-box irreducible diagrams may be important, as confirmed by calculations within the Feynman-Schwinger formalism [12]. Although restricted only to the bound state of scalar particles, ref. [13] showed that some 3-dimensional integral equations conveniently rearrange the series of ladder and crossed-ladder diagrams, equivalently to the BS equation beyond the ladder approximation. One of those 3-dimensional integral equations is the spectator equation.

2.3 Spectator Equation for Fermions

In the spectator equation the restriction on the energy integration variable is motivated by important cancellations between box and crossed-box amplitudes. For scalar-interacting particles in the one-body limit the above cancellation is exact order by order [5, 11]. Also, when one of the masses is much larger than the other, the spectator equation in the ladder approximation alone gives practically the same result as the full Bethe-Salpeter equation, as shown in ref. [14]. This shows the efficiency gained in the rearrangement of the meson-exchange series, prior to its truncation. Furthermore, it has been shown that for nucleons (with equal masses) the non-vanishing difference between the sum of box and crossed-box diagrams and the spectator ladder diagrams can be effectively represented by one-heavier-boson exchanges [15]. The spectator equation, with an appropriate OBE kernel, is therefore suitable for applications to the two- and three-nucleon systems, as successfully done in refs. [2, 6, 16, 17].

In order to satisfy the Pauli principle the spectator formalism consists of a set of two coupled equations, as introduced in ref. [6]. Since here we evaluate the scattering amplitude with both particles on-mass-shell in the initial state, the two equations reduce to a single one.

Following ref. [6], the scattering equation corresponding to the amplitude, where particle 1 is on-mass-shell in the initial and final states, is written as

$$\mathcal{M}_{\alpha'\beta',\alpha\beta}(p',p;P) = \bar{\mathcal{V}}_{\alpha'\beta',\alpha\beta}(p',p;P) - \frac{1}{2}\sum_{\substack{\alpha_1,\alpha_2\\ \beta_1,\beta_2}} \int \frac{d^3k}{(2\pi)^3}\frac{m}{E_{\mathbf{k}}}\bar{\mathcal{V}}_{\alpha'\beta',\alpha_1\beta_1}(p',k;P) \times G_{\alpha_1\beta_1,\alpha_2\beta_2}(k;P)\mathcal{M}_{\alpha_2\beta_2,\alpha\beta}(k,p;P), \tag{2.1}$$

where

$$\bar{\mathcal{V}}_{\alpha'\beta',\alpha\beta}(p',p;P) = \mathcal{V}_{\alpha'\beta',\alpha\beta}(p',p;P) + (-1)^I \mathcal{V}_{\beta'\alpha',\alpha\beta}(-p',p;P) \tag{2.2}$$

is the anti-symmetrized interaction kernel. The variable I denotes the total isospin of the two-nucleon system. The notation uses m for the nucleon mass, p and p' for the relative initial and final four-momenta, and P for the total four-momentum. Also, the indexes that represent the Dirac components of particles 1 and 2 are, respectively, α' and β' for the final state, and α and β for the initial state. The on-mass-shell energy corresponding to the three-momentum $\mathbf{k}$ is $E_{\mathbf{k}} = \sqrt{m^2 + \mathbf{k}^2}$. We considered the c.m. reference frame, where $P = (W, 0)$ (W is the total energy). In terms of the relative momentum k the momenta of particles 1 and 2 are given by $k_1 = P/2 + k$ and $k_2 = P/2 - k$, respectively. When both particles are on-mass-shell the relative three-momentum is represented by $\bar{\mathbf{p}}$ and then $W = 2E_{\bar{\mathbf{p}}}$.

In Eq. (2.1) $G_{\alpha_1\beta_1,\alpha_2\beta_2}(k;P)$ is the two-nucleon spectator-formalism propagator and is given by

$$G_{\alpha_1\beta_1,\alpha_2\beta_2}(k;P) = \Lambda_{\alpha_1\alpha_2}(P/2+k) G_{\beta_1\beta_2}(P/2-k), \tag{2.3}$$

where $\Lambda_{\alpha_1\alpha_2}(k_1)$ is the particle-1 positive-energy projector and $G_{\beta_1\beta_2}(k_2)$ the particle-2 Dirac propagator. The asymmetry due to the propagator G is only apparent, since the anti-symmetrization is guaranteed by the form of the kernel in Eq. (2.2).

Following the formalism introduced in ref. [6], we write the scattering amplitude in terms of the helicity and the $(+,-)$ energy components (ρ-spin) by defining

$$\begin{aligned}\mathcal{M}^{\rho_1'\rho_2',\rho_1\rho_2}_{\lambda_1'\lambda_2',\lambda_1\lambda_2}(p',p;P) = \sum_{\substack{\alpha',\beta' \\ \alpha,\beta}} \bar{u}^{\rho_1'}_{\alpha'}(p_1',\lambda_1') \bar{u}^{\rho_2'}_{\beta'}(p_2',\lambda_2') \mathcal{M}_{\alpha'\beta',\alpha\beta}(p',p;P) \\ \times u^{\rho_1}_{\alpha}(p_1,\lambda_1) u^{\rho_2}_{\beta}(p_2,\lambda_2),\end{aligned} \tag{2.4}$$

(this definition differs from the one in ref. [6] in the multiplicative kinematical factor $(m/E_{\mathbf{p}'})(m/E_{\mathbf{p}})$), where $u^{\pm}_{\alpha}(p_j,\lambda)$ ($j = 1,2$) stands for the Dirac components of the asymptotic states of particles j (see Appendix A), λ_1 (λ_1') and λ_2 (λ_2') are the initial (final) helicities for particles 1 and 2, respectively. The indexes ρ_j and ρ_j' with $j = 1,2$ express the initial and final ρ-spin states for particle j. A similar expression holds for $\bar{\mathcal{V}}$.

The scattering amplitude in terms of the helicity and ρ-spin states reads finally

$$\begin{aligned}\mathcal{M}^{+\rho_2',+\rho_2}_{\lambda_1'\lambda_2',\lambda_1\lambda_2}(p',p;P) = \bar{\mathcal{V}}^{+\rho_2',+\rho_2}_{\lambda_1'\lambda_2',\lambda_1\lambda_2}(p',p;P) - \sum_{\rho,\lambda_3,\lambda_4} \int \frac{d^3k}{(2\pi)^3} \bar{\mathcal{V}}^{+\rho_2',+\rho}_{\lambda_1'\lambda_2',\lambda_3\lambda_4}(p',k;P) \\ \times g^{\rho}(k;W) \mathcal{M}^{+\rho,+\rho_2}_{\lambda_3\lambda_4,\lambda_1\lambda_2}(k,p;P),\end{aligned} \tag{2.5}$$

where the positive and negative energy components of the propagator are

$$g^{+}(k;W) = \frac{1}{2}\left(\frac{m}{E_{\mathbf{k}}}\right)^2 \frac{1}{2E_{\mathbf{k}} - W - i\varepsilon}, \tag{2.6}$$

$$g^{-}(k;W) = -\frac{1}{2}\left(\frac{m}{E_{\mathbf{k}}}\right)^2 \frac{1}{W}. \tag{2.7}$$

The component (2.6) of the nucleon propagator presents a pole singularity.

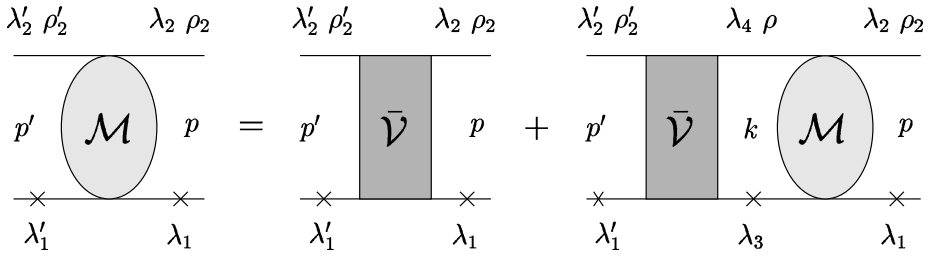

Fig. 1. Helicity representation of the spectator equation. The crosses on the lines mean that the corresponding particles are on-mass-shell with positive energy

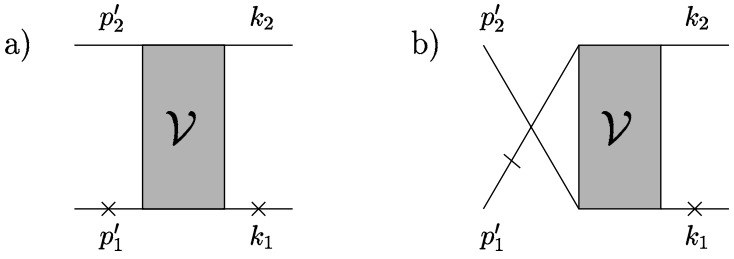

Fig. 2. (**a**) Direct term of the kernel $\bar{\mathcal{V}}$. (**b**) Exchange term of the kernel $\bar{\mathcal{V}}$

In the spectator formalism one of the particles is always on-mass-shell in a positive-energy state and henceforth in Eq. (2.5) there is always a positive ρ-spin state in the initial, intermediate, and final states. The diagrammatic representation of Eq. (2.5) is given in Fig. 1. The kernel $\bar{\mathcal{V}}$ contains two terms, the direct term and the exchange term (see Eq. (2.2)), which are represented in Fig. 2.

In this work we use an OBE kernel including π, σ, ρ, and ω meson exchanges. The model used for the kernel is very similar to the one of refs. [6, 16]. For π-exchange we consider a mixture of pseudo-scalar (PS) and pseudo-vector (PV) couplings in the vertex, defined as

$$\Lambda_\pi(p_j', k_j) = \lambda_\pi \gamma^5 + (1 - \lambda_\pi) \frac{(\not{p}_j' - \not{k}_j)}{2m} \gamma^5, \tag{2.8}$$

where $0 \leq \lambda_\pi \leq 1$ is the admixture parameter, and j specifies the nucleon involved ($j = 1, 2$). Explicit expressions for $\mathcal{V}$ can be found in Appendix B.

The parameters m_π, m_ρ, and m_ω are fixed by the experimental values for physical mesons. The remaining 11 parameters were fitted to the *np* differential cross-section data. These kernel parameters will be presented in Sect. 4.

3 Solution of the Integral Equation Without Partial Wave Decomposition

In order to solve the scattering equation we need to specify the scattering conditions, that is the initial and final momenta. We choose a reference frame where the incoming momentum is along the z-axis and write the initial, final, and intermediate

momenta in terms of spherical coordinates,

$$\mathbf{p} = (\mathrm{p}, 0, 0), \tag{3.1}$$

$$\mathbf{p}' = (\mathrm{p}', \theta', \varphi'), \tag{3.2}$$

$$\mathbf{k} = (\mathrm{k}, \theta, \varphi). \tag{3.3}$$

where $\mathrm{p}' = |\mathbf{p}'|$, $\mathrm{p} = |\mathbf{p}|$, and $\mathrm{k} = |\mathbf{k}|$.

3.1 Integration of the Azimuthal Angle

To perform the φ-integration we need to apply on the scattering amplitude a rotation of an angle φ around the z-axis. In Appendix C we show that

$$\mathcal{M}^{+\rho_2',+\rho_2}_{\lambda_3\lambda_4,\lambda_1\lambda_2}(\mathrm{k},\theta,\varphi;\mathrm{p};W) = \exp\left[i(\lambda_1-\lambda_2)\frac{\varphi}{2}\right]\mathcal{M}^{+\rho_2',+\rho_2}_{\lambda_3\lambda_4,\lambda_1\lambda_2}(\mathrm{k},\theta,0;\mathrm{p};W), \tag{3.4}$$

where the angles $\mathbf{p}$ are omitted for simplicity.

Inserting Eq. (3.4) into the spectator equation (2.5) and taking $\varphi' = 0$ (xz is the reaction plane), we can factorize the φ-dependence obtaining

$$\begin{aligned}\mathcal{M}^{+\rho_2',+\rho_2}_{\lambda_1'\lambda_2',\lambda_1\lambda_2}(\mathrm{p}',\theta',0;\mathrm{p};W) &= \bar{\mathcal{V}}^{+\rho_2',+\rho_2}_{\lambda_1'\lambda_2',\lambda_1\lambda_2}(\mathrm{p}',\theta',0;\mathrm{p};W)\\ &\quad - \sum_{\rho,\lambda_3,\lambda_4}\int\frac{\mathrm{k}^2\,\mathrm{dk}}{2\pi}\int\frac{d\cos\theta}{2\pi}V^{+\rho_2',+\rho}_{\lambda_1'\lambda_2',\lambda_3\lambda_4}(\mathrm{p}',\theta',\mathrm{k},\theta;\bar{\lambda},W)\\ &\quad \times g^{\rho}(\mathrm{k};W)\mathcal{M}^{+\rho,+\rho_2}_{\lambda_3\lambda_4,\lambda_1\lambda_2}(\mathrm{k},\theta,0;\mathrm{p};W),\end{aligned} \tag{3.5}$$

where

$$V^{+\rho_2',+\rho}_{\lambda_1'\lambda_2',\lambda_3\lambda_4}(\mathrm{p}',\theta',\mathrm{k},\theta;\bar{\lambda},W) = \frac{1}{2\pi}\int d\varphi\, e^{i\bar{\lambda}\varphi}\bar{\mathcal{V}}^{+\rho_2',+\rho}_{\lambda_1'\lambda_2',\lambda_3\lambda_4}(\mathrm{p}',\theta',\varphi';\mathrm{k},\theta,\varphi;W) \tag{3.6}$$

and

$$\bar{\lambda} = \frac{\lambda_1-\lambda_2}{2} \tag{3.7}$$

can take the values 0, ± 1.

The scattering equation (3.5) is already a 2-dimensional integral equation and includes the propagator function $g^{\rho}(\mathrm{k};W)$ which has a real pole at $\mathrm{k} = \bar{\mathrm{p}}$ ($W = 2E_{\mathbf{k}}$) for $\rho = +1$. Performing the contour integration we obtain

$$\begin{aligned}&\mathcal{M}^{+\rho_2',+\rho_2}_{\lambda_1'\lambda_2',\lambda_1\lambda_2}(\mathrm{p}',\theta',0;\mathrm{p};W)\\ &\quad = \bar{\mathcal{V}}^{+\rho_2',+\rho_2}_{\lambda_1'\lambda_2',\lambda_1\lambda_2}(\mathrm{p}',\theta',0;\mathrm{p};W) - \sum_{\rho,\lambda_3,\lambda_4}\mathcal{P}\int\frac{\mathrm{k}^2\mathrm{dk}}{2\pi}\int\frac{d\cos\theta}{2\pi}V^{+\rho_2',+\rho}_{\lambda_1'\lambda_2',\lambda_3\lambda_4}(\mathrm{p}',\theta';\mathrm{k},\theta;\bar{\lambda},W)\\ &\qquad \times g^{\rho}_{\varepsilon=0}(\mathrm{k};W)\mathcal{M}^{+\rho,+\rho_2}_{\lambda_3\lambda_4,\lambda_1\lambda_2}(\mathrm{k},\theta,0;\mathrm{p};W)\\ &\qquad - i\frac{m^2\bar{\mathrm{p}}}{4W}\sum_{\lambda_3,\lambda_4}\int\frac{d\cos\theta}{2\pi}V^{+\rho_2',++}_{\lambda_1'\lambda_2',\lambda_3\lambda_4}(\mathrm{p}',\theta';\bar{\mathrm{p}},\theta;\bar{\lambda},W)\mathcal{M}^{++,+\rho_2}_{\lambda_3\lambda_4,\lambda_1\lambda_2}(\bar{\mathrm{p}},\theta,0;\mathrm{p};W).\end{aligned} \tag{3.8}$$

In this equation we use $g^{\rho}_{\varepsilon=0}(\mathrm{k};W)$ to represent the $\varepsilon=0$ limit of $g^{\rho}(\mathrm{k};W)$ (see Eqs. (2.6)–(2.7)). The multiplicative factor of the last term is a result of the residue

$$\frac{1}{2}\left[\frac{1}{2}\left(\frac{m}{E_{\mathbf{k}}}\right)^2\frac{\mathrm{k}^2}{\left|\dfrac{\mathrm{d}}{\mathrm{dk}}(2E_{\mathbf{k}}-W)\right|}\right]_{\mathrm{k}=\bar{\mathrm{p}}}=\frac{m^2\bar{\mathrm{p}}}{4W}. \tag{3.9}$$

In Eq. (3.8) only the function $g^{+}(\mathrm{k};W)$ has a singularity, but we include the principal-part symbol $\mathcal{P}$ also for $\rho=-1$ for the sake of simplicity.

The φ-integration (3.6) can be performed either analytically or numerically. In refs. [3, 4, 7–9] the numerical integration was made. Here we choose the analytical integration in order to minimize computing time.

The analytical expressions depend on the kernel structure. In particular, the complexity of the analytical expressions depends crucially upon the form factors (see Sect. 3.4). Relatively simple results are obtained, nevertheless, for the monopolar choice of the meson-nucleon form factors. In this case we can write Eq. (3.6) as

$$\int d\varphi\, e^{i\bar{\lambda}\varphi}\mathcal{V}^{+\rho_2',+\rho_2}_{\lambda_1'\lambda_2',\lambda_3\lambda_4}(p',p;P)=\sum_{\Gamma}C_{\Gamma}\int d\varphi\frac{e^{i\Gamma\varphi}}{(a-b\cos\varphi)(c-b\cos\varphi)^2}, \tag{3.10}$$

where $\Gamma=0,\ \pm1,\ \pm2$, and C_{Γ} is a known function of the momentum magnitudes and the polar angle. Any term of the last equation is subsequently easily integrated over. Meanwhile, in ref. [18], where the equation for πN scattering is solved also without PWD, the authors used the same analytical technique but for an integrand not including form factors. Details of the analytical structure of the kernel can be found in Appendix B and the main steps for the analytical integration are given in Appendix D.

3.2 Numerical Method: Padé Method

For clarity, in the following, the relevant variables in the scattering equation (3.8) are labeled in a simpler and more condensed notation, where we denote each of the eight possible helicity and ρ-spin combinations by a single index $I'=\{\rho_2',\lambda_1',\lambda_2'\}$, $I_k=\{\rho,\lambda_3,\lambda_4\}$, and $I_0=\{\rho_2,\lambda_1,\lambda_2\}$, according to Table 1 ($I'$, I_k, and I_0 have nothing to do with the total isospin I); we omit also the total energy W, the incoming momentum p, and the total isospin I-dependences and perform the

Table 1. Table defining the indexes I_0, I_k, or I'

I_0	ρ	λ_1	λ_2
1	+	−	−
2	+	−	+
3	+	+	−
4	+	+	+
5	−	−	−
6	−	−	+
7	−	+	−
8	−	+	+

following substitutions,

$$\mathcal{M}^{+\rho_2',+\rho_2}_{\lambda_1'\lambda_2',\lambda_1\lambda_2}(\mathrm{p}',\theta',0;\mathrm{p};W) \to \mathcal{M}_{I',I_0}(\mathrm{p}',u),$$
$$\bar{\mathcal{V}}^{+\rho_2',+\rho_2}_{\lambda_1'\lambda_2',\lambda_1\lambda_2}(\mathrm{p}',\theta',0;\mathrm{p};W) \to \bar{\mathcal{V}}_{I',I_0}(\mathrm{p}',u),$$
$$V^{+\rho_2',+\rho}_{\lambda_1'\lambda_2',\lambda_3\lambda_4}(\mathrm{p}',\theta';\mathrm{k},\theta;\bar{\lambda},W) \to V_{I',I_k}(\mathrm{p}',u;\mathrm{k},v),$$

where

$$u = \cos\theta', \tag{3.11}$$
$$v = \cos\theta. \tag{3.12}$$

Thus, Eq. (3.8) reads

$$\begin{aligned}\mathcal{M}_{I',I_0}(\mathrm{p}',u) &= \bar{\mathcal{V}}_{I',I_0}(\mathrm{p}',u)\\ &\quad - \sum_{I_k=1}^{8}\mathcal{P}\int_0^\infty \frac{\mathrm{k}^2\,\mathrm{dk}}{2\pi}\int_{-1}^{1}\frac{dv}{2\pi}V_{I',I_k}(\mathrm{p}',u;\mathrm{k},v)g^{I_k}(\mathrm{k};W)\mathcal{M}_{I_k,I_0}(\mathrm{k},v)\\ &\quad - i\frac{m^2\bar{\mathrm{p}}}{4W}\sum_{I_k=1}^{4}\int_{-1}^{1}\frac{dv}{2\pi}V_{I',I_k}(\mathrm{p}',u;\bar{\mathrm{p}},v)\mathcal{M}_{I_k,I_0}(\bar{\mathrm{p}},v),\end{aligned} \tag{3.13}$$

with

$$g^{I_k}(\mathrm{k};W) = \begin{cases} g^+_{\varepsilon=0}(\mathrm{k};W) & \text{if} \quad I_k = 1,\ldots,4,\\ g^-(\mathrm{k};W) & \text{if} \quad I_k = 5,\ldots,8.\end{cases} \tag{3.14}$$

In order to obtain a numerical solution of Eq. (3.13) we carry out a discretization of the integral variables, $\mathrm{k}\in[0,+\infty[$ and $v\in[-1,1]$, and use a Gaussian quadrature-integration technique. We choose a grid of N_p+1 points for all momenta, p', k, and p, and a grid of N_u+1 points for the angular variables u and v. With this discretization procedure we transform the integral equation (3.8) into an algebraic set of equations

$$M = V + C\cdot M, \tag{3.15}$$

where M and V are the matrix vectors $\mathcal{M}_{I',I_0}(k_{i'},v_{j'})$ and $\bar{\mathcal{V}}_{I',I_0}(k_{i'},v_{j'})$. The C-matrix can be decomposed as $C=A+B$. For $I_k=1,\ldots,4$, we have

$$A_{(I'i'j'),(I_kij)} = -\frac{w_i'h_j}{(2\pi)^2}k_i^2V_{I',I_k}(k_{i'},u_{j'};k_i,u_j)g^+(k_i;W), \tag{3.16}$$

$$B_{(I'i'j'),(I_kij)} = -\frac{h_j}{(2\pi)^2}\frac{m^2\bar{\mathrm{p}}}{2}\left(i\frac{\pi}{W}-\Delta S\right)V_{I',I_k}(k_{i'},u_{j'};\bar{\mathrm{p}},u_j)\delta_{i,N_p+1}, \tag{3.17}$$

with

$$\Delta S = S - S', \tag{3.18}$$

$$S = \mathcal{P}\int_0^{+\infty}dk\,\frac{k}{E_{\mathbf{k}}^2}\frac{1}{2E_{\mathbf{k}}-W} = -\frac{1}{W}\log\frac{W-2m}{2m}, \tag{3.19}$$

$$S' = \sum_{i=1}^{N_p}w_i'\frac{k_i}{E_{k_i}^2}\frac{1}{2E_{k_i}-W}. \tag{3.20}$$

For $I_k = 5, \ldots, 8$, we have

$$A_{(I'i'j'),(I_kij)} = -\frac{w'_i h_j}{(2\pi)^2} k_i^2 V_{I',I_k}(k_{i'}, u_{j'}; k_i, u_j) g^-(k_i; W), \tag{3.21}$$

$$B_{(I'i'j'),(I_kij)} = 0. \tag{3.22}$$

In the previous equations w'_i and h_j are the Gaussian weights for the variables k_i and u_j, respectively. The momentum grid is obtained from an $x_i \in]0, 1[$ grid by a change of variables,

$$k_i = \Lambda \frac{x_i}{1 - x_i},$$

where typically we take $\Lambda \simeq 0.5\, m$. In order to determine the on-mass-shell forward scattering amplitude we add the mesh points $k_{N_p+1} = \overline{\mathrm{p}}$ and $u_{N_u+1} = 1$ with zero weight.

The dimension of the above matrices is $n = 8(N_p + 1)(N_u + 1)$, which is a large number when N_p and N_u are of the order of 20. Therefore, a standard matrix-inversion method requiring a large computer memory (for double-precision complex numbers) becomes impracticable. To overcome this limitation we use instead the Padé method, which gives a fast estimate of the result of the Born series for the coupled set of equations,

$$M = \lambda V + \lambda C \cdot M, \tag{3.23}$$

where the parameter λ is introduced by convenience and set to 1 at the end of the calculation. The usual power expansion for $2N + 1$ terms is

$$M = \lambda M^{(1)} + \lambda^2 M^{(2)} + \lambda^3 M^{(3)} + \cdots + \lambda^{2N+1} M^{(2N+1)}. \tag{3.24}$$

The vectors $M^{(i)}$ are evaluated by

$$M^{(1)} = V, \tag{3.25}$$

$$M^{(i+1)} = C \cdot M^{(i)}, \tag{3.26}$$

and any element m of the vector M, given by

$$m = \lambda m_1 + \lambda^2 m_2 + \lambda^3 m_3 + \cdots + \lambda^{2N+1} m_{2N+1}, \tag{3.27}$$

is approximated by a rational function of λ,

$$m_{\text{Padé}}(\lambda) = \lambda \frac{a_0 + \lambda a_1 + \cdots + \lambda^N a_N}{1 + \lambda b_1 + \cdots + \lambda^N b_N}, \tag{3.28}$$

where the $2N + 1$ coefficients a_l and b_l are determined through the $2N + 1$ coefficients m_l, from equating Eqs. (3.27) and (3.28). This method is known in the literature as SPA (scalar Padé approximant) [19] and $m_{\text{Padé}}$ denotes the Padé $[N, N]$ result.

The advantage of the Padé method is that it replaces the matrix inversion by a fast estimate of the Born expansion, where all terms are evaluated as a matrix-vector multiplication. This multiplication can be performed as n dot-products of two vectors of n dimension. Therefore the calculation requires memory to allocate only $2n$, instead of n^2, complex numbers. This reduces substantially the dimension of the problem. The price to pay is the recalculation of the matrix lines.

As we will see in the following section, 11 to 15 Padé terms are needed for convergence. For typical values $N_p = 20$ and $N_u = 30$, the full calculation takes less than 4 minutes in a Pentium 4 at 3.2 GHz, provided that a minimum of 500 GB disk space is available.

3.3 Prescription for Handling the Singularities in the Exchange Kernel

The direct and the exchange kernel differ in the transferred momentum: q in direct kernel; $\hat{q}$ in exchange kernel. In Appendix E we give the expressions for the momentum transfer involved in each of the two terms, and which determine the possible numerical singularities coming from the meson propagators, which need to be taken into account numerically. While the direct term in the kernel of the spectator equation has no singularities in the meson propagators (one has always $\mu^2 - q^2 > 0$), the exchange term, introduced as a consequence of anti-symmetrization, has the singularity corresponding to an on-mass-shell exchanged meson ($\mu^2 = \hat{q}^2$). This singularity condition $\mu^2 = \hat{q}^2$ means the production of a real meson from the off-mass-shell nucleon states. However, since a real meson-production process is not allowed below the pion-production threshold, the associated singularity of $\widehat{\mathcal{V}}$ has no physical correspondence in reality. As shown by Gross et al. this spurious singularity is canceled by higher-order diagrams [6].

In the numerical applications of the spectator equations two prescriptions were considered so far to deal with the spurious singularities [6]:

– *Principal-part prescription*: The singularity is included but only the principal part of the integral is kept. This corresponds to the replacement

$$\int \frac{1}{\mu^2 - \hat{q}^2 - i\varepsilon} \to \mathcal{P}\int \frac{1}{\mu^2 - \hat{q}^2} = \int \left(\frac{1}{\mu^2 - \hat{q}^2 - i\varepsilon} - i\pi\delta\big(\mu^2 - \hat{q}^2\big) \right),$$

where

$$-\hat{q}^2 = (\mathbf{p}' + \mathbf{k})^2 - (E_{\mathbf{p}'} + E_{\mathbf{k}} - W)^2. \tag{3.29}$$

– *Energy-independent prescription*: The momentum transfer is modified in order to remove the singularity. This amounts to the replacement

$$\hat{q} = p_1' - k_2 \to q = p_1' - k_1,$$

or

$$-\hat{q}^2 \to (\mathbf{p}' - \mathbf{k})^2 - (E_{\mathbf{p}'} - E_{\mathbf{k}})^2.$$

This last prescription was preferred in recent applications [6, 16]: The momentum transfer is the same for the propagator in both direct and exchange diagrams, leaving the meson-propagator denominator independent of the two-nucleon-system energy W.

Nevertheless, we introduce here an alternative adopted by us in the present numerical work, which we label the *on-mass-shell prescription*. To understand it, note that Eq. (3.29) can be rewritten as follows [6],

$$-\hat{q}^2 = (\mathbf{p}' + \mathbf{k})^2 - (E_{\mathbf{p}'} - E_{\mathbf{k}})^2 - (W - 2E_{\mathbf{p}'})(W - 2E_{\mathbf{k}}). \tag{3.30}$$

It is the last term of this equation which generates the spurious singularities mentioned, while vanishing when both particles are on-mass-shell either in the initial state ($W = 2E_{\mathbf{k}}$) or in the final state ($W = 2E_{\mathbf{p}'}$). We therefore define the *on-mass-shell prescription* by taking for $-\hat{q}^2$ the expression

$$-\hat{q}^2 \to (\mathbf{p}' + \mathbf{k})^2 - (E_{\mathbf{p}'} - E_{\mathbf{k}})^2. \tag{3.31}$$

With this choice the exchange kernel $\widehat{\mathcal{V}}$ is consistent with the Feynman rules in the on-mass-shell limit. This is a physical argument in favor of our choice. Furthermore, Eq. (3.31) implies that when the direct term in a particular interaction is dominant in the forward direction, then the exchange term dominates in the backward direction, as it happens for interactions mediated by scalars. We point out that this property is not satisfied by the *energy-independent prescription*. Note, however, that the *on-mass-shell prescription* is also energy-independent.

3.4 Strong Form Factors Required by the 3D Numerical Method

Mathematically, form factors provide the necessary regularization of the integrals for the high-order loops. Since in this work we solve the scattering equation without partial wave expansion, a careful study of the integrand function had to be performed, in order to determine form-factor functions adequate for the convergence of the method used.

The starting point for the choice of form factors per vertex was the decomposition suggested by Gross and Riska [20],

$$F_i(p'_j, k_j) = f_{m_i}(q^2) f_N(p'^2_j) f_N(k_j^2), \tag{3.32}$$

where p'_j (k_j) is the final (initial) momentum of the nucleon j ($j = 1, 2$), $q = p'_j - k_j$ is the transfer momentum, f_{m_i} is the form factor of meson i and f_N the nucleon form factor.

For the meson form factor our choice is

$$f_{m_i}(q^2) = \frac{\Lambda_{m_i}^2}{\Lambda_{m_i}^2 - q^2}, \tag{3.33}$$

where Λ_{m_i} is the cut-off of meson i. Note that by construction the functions $f_{m_i}(q^2)$ only modify the kernel for large q^2 (for $q^2 = 0$ we have $f_{m_i}(q^2) = 1$), and therefore do not suppress the large momentum dependence of $\mathcal{V}(k, k; P)$.

For the form factors f_N we take

$$f_N(k_j^2) = \left[\frac{\tilde{\Lambda}_N^2}{\tilde{\Lambda}_N^2 + (m^2 - k_j^2)^2} \right]^n, \tag{3.34}$$

with

$$\tilde{\Lambda}_N^2 = \Lambda_N^2 - m^2, \tag{3.35}$$

Λ_N being the nucleon cut-off. These functions f_N regulate the asymptotic behavior of both $\mathcal{V}(k, k; P)$ and $\mathcal{V}(k, p; P)$, and are normalized to 1 at the on-mass-shell condition. For the meson exchange diagrams that enter the kernel of the integral

equation one of the nucleons is always on-mass-shell, and therefore the contribution from the corresponding function f_N is 1.

The factorization (3.32) has been applied in the spectator equation [6, 16] and also used in the quasi-potential framework without retardation (where $k = (0, \mathbf{k})$) [21]. In the present calculation we found that in order to solve the spectator equation with 3D methods the value $n = 1$ in Eq. (3.34), used in previous applications with PWD [16], was not large enough for the numerical convergence of $\mathcal{M}(k, p; P)$. We had to take instead $n = 2$. This is mostly due to the meson-propagator behavior which peaks for forward and backward scattering angles at high values of the momentum [22]. Using the PWD method the meson-propagator peak is smeared by the angle integration, but in the 3D method the structure of the propagator cannot be smoothened.

3.5 Properties and Symmetries of the Amplitudes

Using parity, time reversal, and particle-interchange symmetries we can decrease the number of independent amplitudes [23, 24]. In particular, parity invariance reduces the 16 helicity amplitudes of Eq. (2.5) with $\rho' = +1$, $\rho = +1$ to 8 independent ones, according to

$$M_1 = \mathcal{M}_{++,++}(\mathrm{p}', u; \mathrm{p}, 1) = \mathcal{M}_{--,--}(\mathrm{p}', u; \mathrm{p}, 1), \tag{3.36}$$

$$M_2 = \mathcal{M}_{--,++}(\mathrm{p}', u; \mathrm{p}, 1) = \mathcal{M}_{++,--}(\mathrm{p}', u; \mathrm{p}, 1), \tag{3.37}$$

$$M_3 = \mathcal{M}_{+-,+-}(\mathrm{p}', u; \mathrm{p}, 1) = \mathcal{M}_{-+,-+}(\mathrm{p}', u; \mathrm{p}, 1), \tag{3.38}$$

$$M_4 = \mathcal{M}_{-+,+-}(\mathrm{p}', u; \mathrm{p}, 1) = \mathcal{M}_{+-,-+}(\mathrm{p}', u; \mathrm{p}, 1), \tag{3.39}$$

$$M_5 = \mathcal{M}_{-+,++}(\mathrm{p}', u; \mathrm{p}, 1) = -\mathcal{M}_{+-,--}(\mathrm{p}', u; \mathrm{p}, 1), \tag{3.40}$$

$$M_6 = \mathcal{M}_{+-,++}(\mathrm{p}', u; \mathrm{p}, 1) = -\mathcal{M}_{-+,--}(\mathrm{p}', u; \mathrm{p}, 1), \tag{3.41}$$

$$M_7 = \mathcal{M}_{++,+-}(\mathrm{p}', u; \mathrm{p}, 1) = -\mathcal{M}_{--,-+}(\mathrm{p}', u; \mathrm{p}, 1), \tag{3.42}$$

$$M_8 = \mathcal{M}_{--,+-}(\mathrm{p}', u; \mathrm{p}, 1) = -\mathcal{M}_{++,-+}(\mathrm{p}', u; \mathrm{p}, 1). \tag{3.43}$$

In the case $\rho' = -1$ the right-hand side of the equalities includes also the phase $(-1)^{(1-\rho')/2} = -1$.

The above relations are valid either p' is on- or off-mass-shell. Restricting to the on-mass-shell situation, further relations arise,

$$M_7 = M_6, \tag{3.44}$$

$$M_8 = -M_5, \tag{3.45}$$

$$M_5 = -M_6. \tag{3.46}$$

The last identity is valid only for identical particles. As a result we are left with only 5 independent amplitudes. We point out that these relations are independent of the interaction used and of any prescription adopted, and merely result from the symmetries mentioned above. The relations (3.36)–(3.43) were tested numerically as a check to the code, since we did not explicitly impose the symmetries to reduce the number of equations. If we consider, instead, a QP equation of the instantaneous type (no retardation included), e.g., the Blankenbecler-Sugar [25] or the

equal-time [26] equations, we could use more symmetry properties to reduce even further the number of off-mass-shell amplitudes, given that the particles have always the same energy.

Finally we add also that, for equations of the instantaneous type, a convenient combination of the helicity states defines states of well-defined parity and two-body spin and helicity. The use of that basis states reduces the size of the numerical problem by block-diagonalizing the set of equations. This was done for example in refs. [3, 4] in a non-relativistic framework (no $\rho' = -1$ states). Nevertheless, for three-body applications [4] the helicity combination has to be inverted by calculating back the amplitudes in the asymptotic basis of uncoupled helicities.

4 Results and Discussion

In this section we discuss the results obtained from fitting the transition amplitudes to the *np* differential cross section, we show the on- and off-mass-shell amplitudes calculated with the kernel with the fitted parameters, and we present the study of the convergence of the amplitude as a function of the energy.

The numerical results were checked to satisfy the optical theorem

$$\mathrm{Im}[\mathcal{M}^{++,++}_{\lambda_1\lambda_2,\lambda_1\lambda_2}(\bar{\mathbf{p}},1;\bar{\mathbf{p}},1)] = -\frac{m^2\bar{\mathbf{p}}}{4W}\sum_{\lambda_3\lambda_4}\int_{-1}^{1}\frac{dv}{2\pi}\left|\mathcal{M}^{++,++}_{\lambda_3\lambda_4,\lambda_1\lambda_2}(\bar{\mathbf{p}},v;\bar{\mathbf{p}},1)\right|^2. \qquad (4.1)$$

Since the optical theorem only probes the on-mass-shell amplitudes, the results for the off-mass-shell amplitudes were tested by numerically checking that they satisfy the symmetry properties as described in the previous section.

Table 2. Model parameters. The masses are m_m, the coupling constants g_m are redefined as $G_m = g_m^2/4\pi$ ($m = \pi,\ \rho,\ \sigma,\ \omega$) and κ_m is the anomalous magnetic moment of the vector mesons. While Λ_π is the cut-off parameter for the pion, the variable Λ_m stands for the cut-off of the form factors for the other mesons. See Appendix B for the kernel expressions and Sect. 3.4 for the definitions of the form factors

m_π	138 MeV
G_π	13.470
λ_π	0.0
Λ_π	1190 MeV
m_σ	497 MeV
G_σ	3.782
m_ρ	770 MeV
G_ρ	0.100
κ_ρ	5.644
m_ω	783 MeV
G_ω	8.100
κ_ω	0.337
Λ_m	2400 MeV
Λ_N	1783 MeV

4.1 On-Mass-Shell Amplitudes and Differential Cross Section

Asymptotically the state of the two nucleons is characterized by the individual isospin states. Therefore, for the *np* system, we considered

$$T^{np}_{\lambda'_1\lambda'_2,\lambda_1\lambda_2}(\mathrm{p}',u;\mathrm{p},1)=\tfrac{1}{2}T^{10}_{\lambda'_1\lambda'_2,\lambda_1\lambda_2}(\mathrm{p}',u;\mathrm{p},1)+\tfrac{1}{2}T^{00}_{\lambda'_1\lambda'_2,\lambda_1\lambda_2}(\mathrm{p}',u;\mathrm{p},1), \qquad (4.2)$$

where $T^{I0}_{\lambda'_1\lambda'_2,\lambda_1\lambda_2}$ represents the anti-symmetrized matrix $\mathcal{M}$ with a total isospin I ($I_z=0$).

We start by presenting in Table 2 the results for the interaction-kernel parameters that were obtained from the fit of the scattering amplitudes to the *np* differential cross section. In the pion-exchange-diagram contribution to the kernel we let

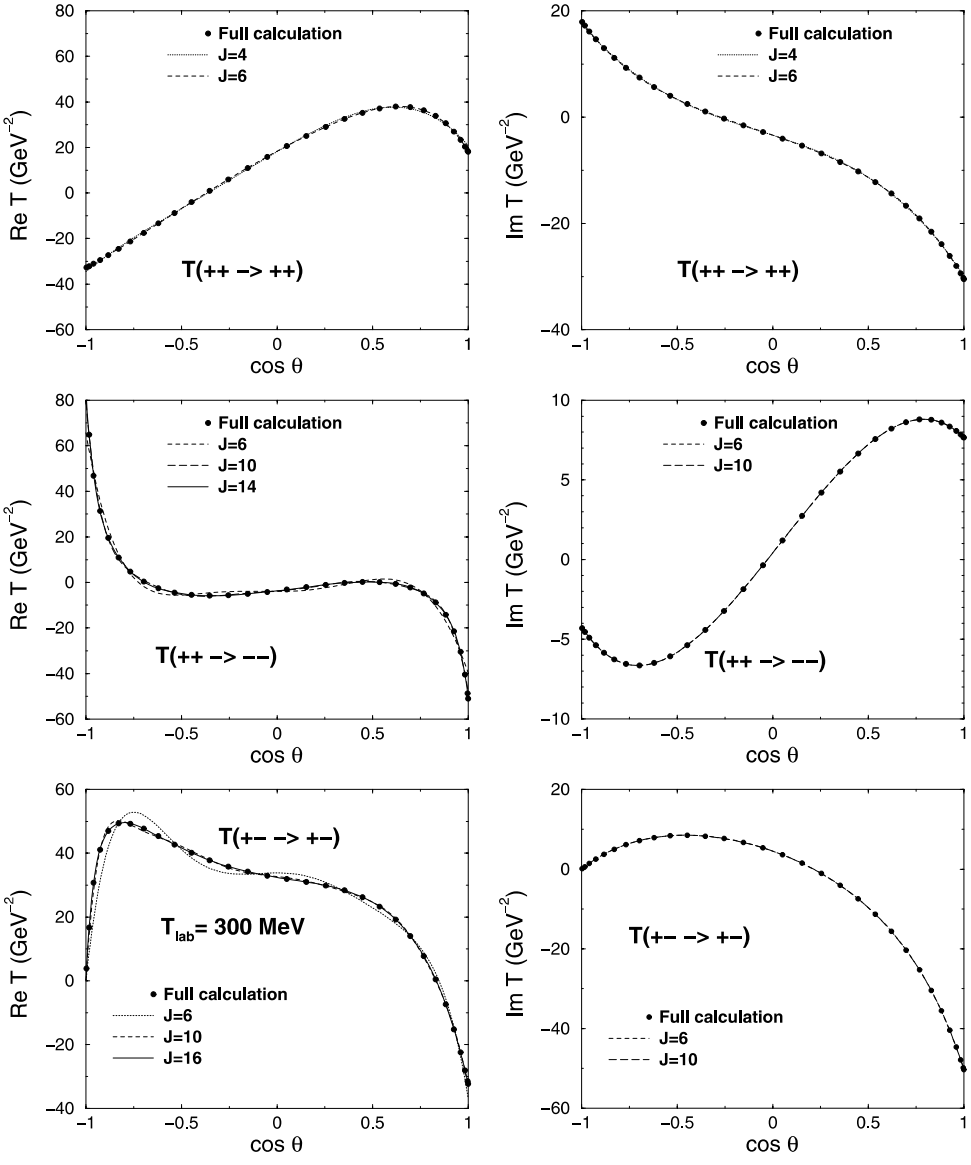

Fig. 3. Helicity amplitudes for 300 MeV and partial wave decomposition

the PS-PV admixture parameter to float during the fit, and the best fit was obtained for $\lambda_\pi = 0$, which corresponds to PV coupling. As for the cut-off parameters, we also allowed Λ_π to be different from Λ_m (with m referring to all the other mesons). In the spectator-equation *NN* model described in ref. [6], all cut-off parameters are taken to be the same. In ref. [16], an update of the *NN* model is reported where a different cut-off singled out the pion-exchange part of the OBE (one-boson-exchange) interaction. We followed the latter approach since we consider that it is more consistent with the idea of the special role of the pion in the nuclear interaction, and the associated interpretation of the effective heavy meson exchanges as a regularization of its behavior in the large-momentum region (short-range in configuration space). The larger value obtained in the fit for the cut-off of all mesons different from the pion is therefore a natural and expected result. *A posteriori* it serves as a consistency check of that underlying assumption of the OBE models: Compared to the pion, the effective heavy mesons are supposed to be important in the large momentum range. Were their cut-off momenta smaller or of similar size as the pion cut-off momentum, this could not be the case.

Figs. 3 and 4 show the scattering amplitudes (both real and imaginary parts) obtained, at a fixed energy $T_{\rm lab} = 300\,\text{MeV}$, for all independent helicity channels. The comparison between the exact result and the PWD results with increasing values of the maximum total angular momentum included is shown.

The convergence of the Padé amplitudes has been carefully examined, and the iteration procedure stopped when both real and imaginary parts of T converge with

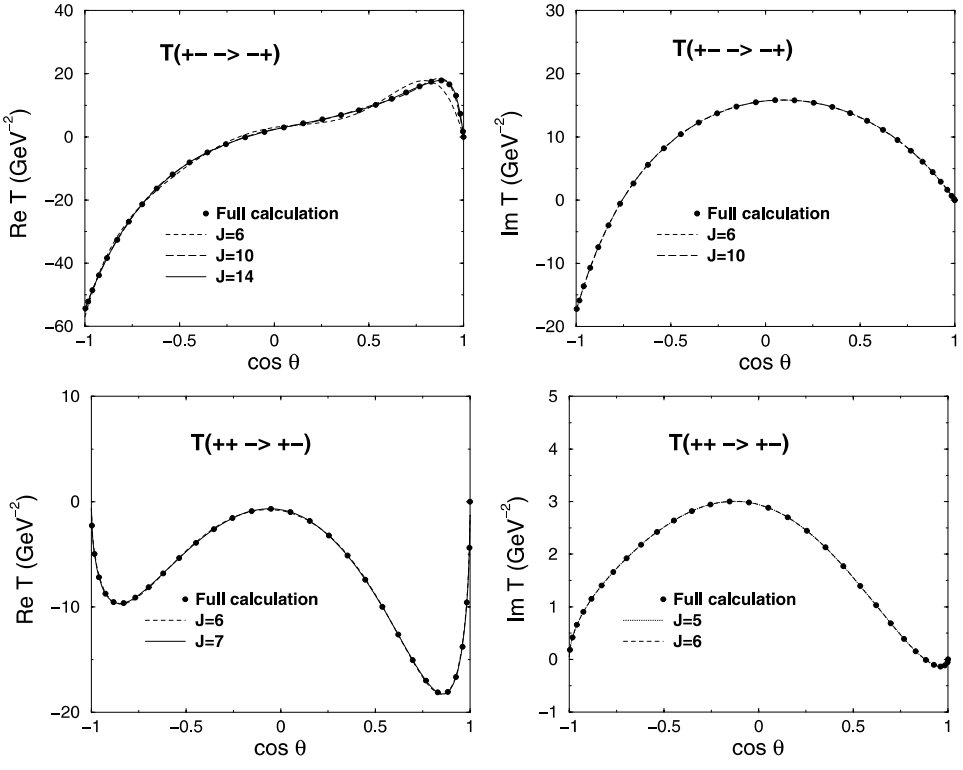

Fig. 4. Helicity amplitudes for 300 MeV and partial wave decomposition

a relative error lower than 10^{-2}. In general, we conclude that grids with $N_p = N_u = 20$ were sufficient below 200 MeV for the numerical convergence of the solution. For 300 MeV we use $N_u = 30$. Here one may think that this number of grid points, as implied by the polar-angle discretization, leads to a numerical problem about the same size of the one of the partial wave-expansion case. However, we emphasize that:

- The polar angle dependence in the *NN* potential factorizes as given in Appendix D. This straightforwardly allows for an optimization of the CPU time of the calculation, which, however, is impossible in the PWD of the potential. There, for each momentum case, the integration on that angle has to be re-calculated.
- The accuracy of PWD decreases with increasing partial-wave index, due to the form of the Legendre polynomials. This limits the precision of the PWD method at high energies for applications in *NN* scattering, where the number of partial waves increases with energy, as evidenced by the three-body calculations in ref. [3].
- In the *NN* scattering problem the number of partial waves needed for the PWD convergence increases with the energy, however, the number of mesh points in the 3D calculation does not increase significantly with energy.

For the helicity $\lambda_1\lambda_2 = +-$ channel, convergence requires 13 Padé terms for $I = 0$ and 11 terms for $I = 1$. For the $\lambda_1\lambda_2 = ++$ channel 15 terms for $I = 0$ and 13 terms for $I = 1$ are necessary. In all cases the optical theorem was always satisfied with a relative error smaller than 10^{-2}.

After calculating all the on-mass-shell polarized amplitudes we evaluated the differential cross section,

$$\frac{d\sigma}{d\Omega}(\bar{\mathrm{p}}, u) = \frac{1}{(2\pi)^2}\frac{m^4}{W^2}\overline{|T^{np}(\bar{\mathrm{p}}, u)|^2}. \tag{4.3}$$

In this equation $\overline{|T^{np}|^2}$ is given by

$$\overline{|T^{np}(\bar{\mathrm{p}}, u)|^2} = \frac{1}{4}\sum_{\substack{\lambda_1', \lambda_2' \\ \lambda_1, \lambda_2}} |T^{np}_{\lambda_1'\lambda_2', \lambda_1\lambda_2}(\bar{\mathrm{p}}, u; \bar{\mathrm{p}}, 1)|^2, \tag{4.4}$$

an average over the initial helicity states and a sum of the final ones. In Fig. 5 the fit of the *NN* potential model to the differential cross-section *np* data at energies $T_{\mathrm{lab}} = 99,\ 200$, and 319 MeV is shown. Data are collected from the Nijmegen data basis [27] and correspond to refs. [28–30].

At least for the two first energies the quality of the fit is very good. The $T_{\mathrm{lab}} = 319$ MeV energy case is already above the pion production threshold, which justifies the slight decrease of the quality of the fit. Nevertheless, we conclude that the method developed in the present work is reliable and promising. Another point worth mentioning is that the fit selects the PV pion-nucleon coupling (mixing parameter $\lambda_\pi = 0$), in agreement with requirements from chiral symmetry.

4.2 Off-Mass-Shell Amplitudes

The off-mass-shell $T^{np}_{\lambda_1'\lambda_2', \lambda_1\lambda_2}(\mathrm{p}', u; \bar{\mathrm{p}}, 1)$ amplitudes may be plotted as functions of 2 variables in momentum space.

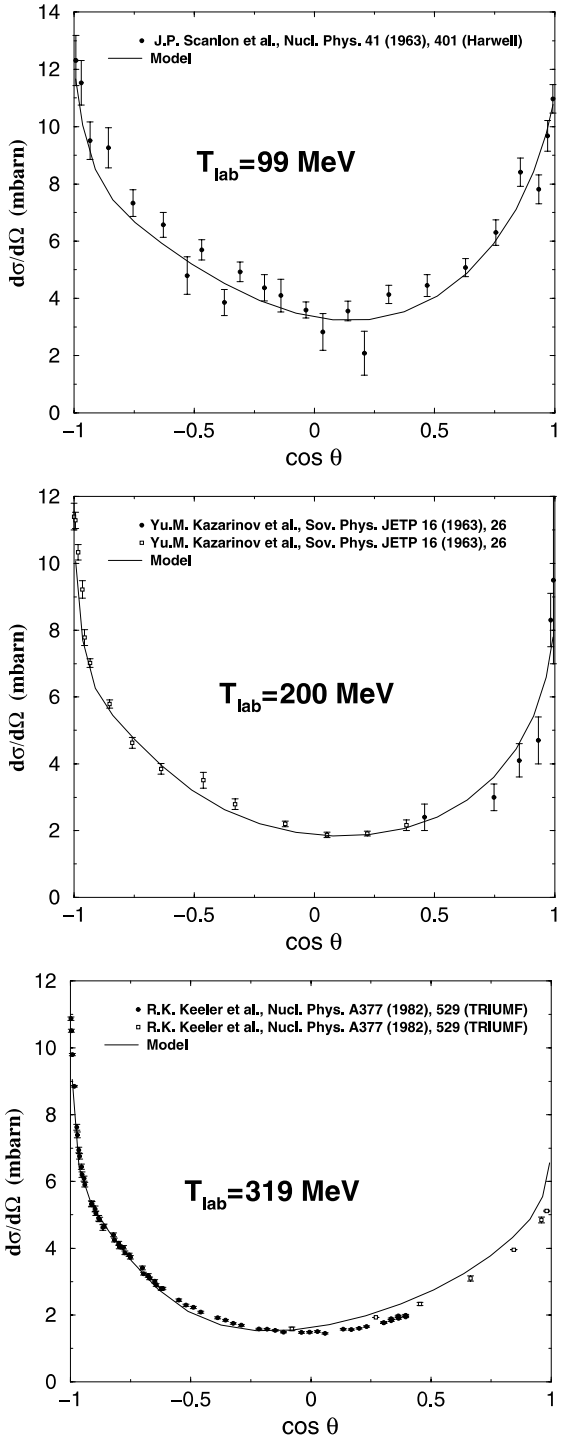

Fig. 5. Differential cross-section results for 99, 200, and 319 MeV

The results for the 8 $\rho' = +1$ amplitudes are presented in Figs. 6 and 7 for $T_{\text{lab}} = 300\,\text{MeV}$. The plots for the $\rho' = -1$ amplitudes are presented in Figs. 8 and 9. Note that the on-mass-shell region corresponds to the line $\text{p}' = 0.375\,\text{GeV}/c$.

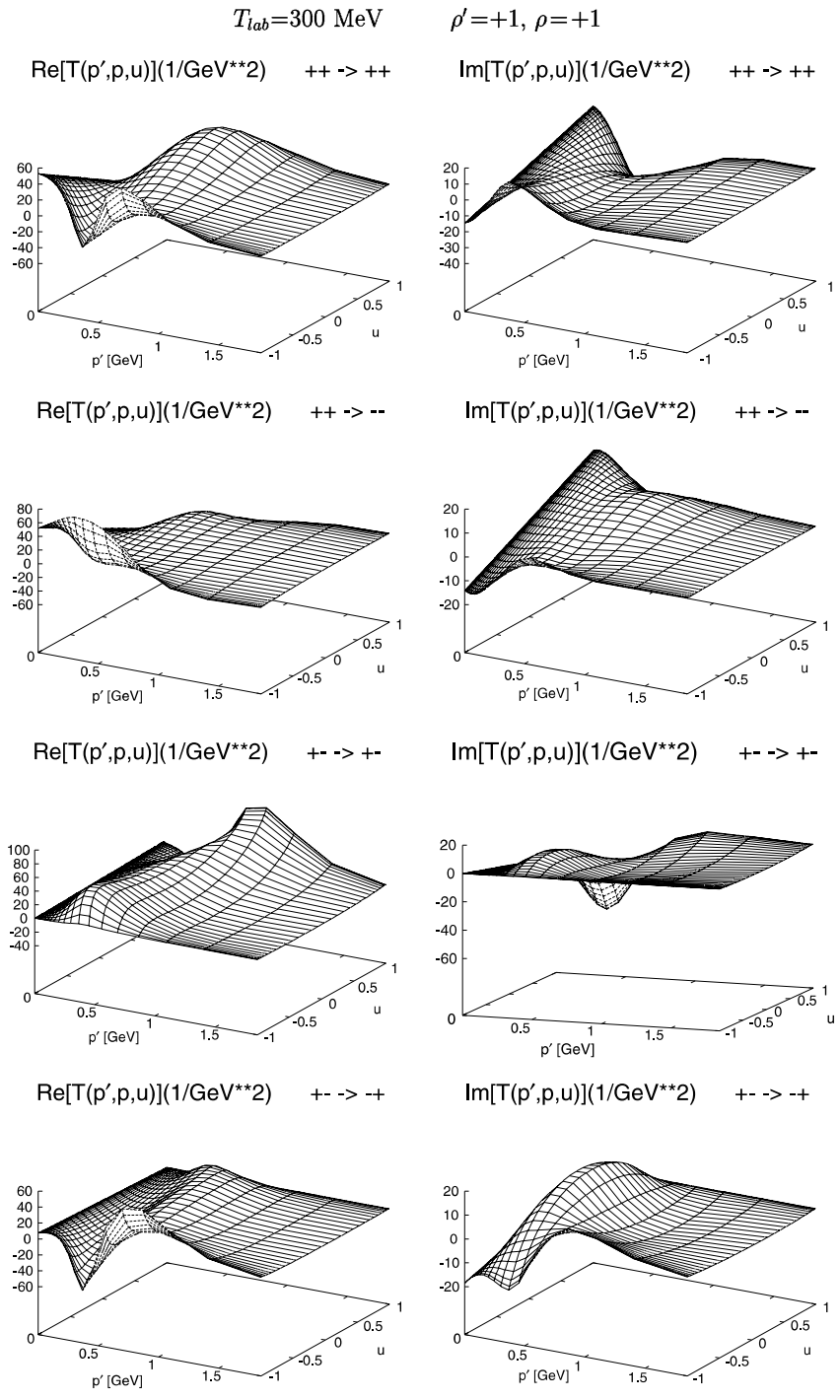

Fig. 6. Off-mass-shell amplitudes for the *np* process with $\rho = +1, \rho' = +1$

The magnitudes of some amplitudes are important up to momenta of the order $1.5\,\mathrm{GeV}/c$, much larger than the on-mass-shell momentum.

It is also important to point out that the amplitudes involving transitions to negative-energy states, $\rho' = -1$, have magnitudes of the same order

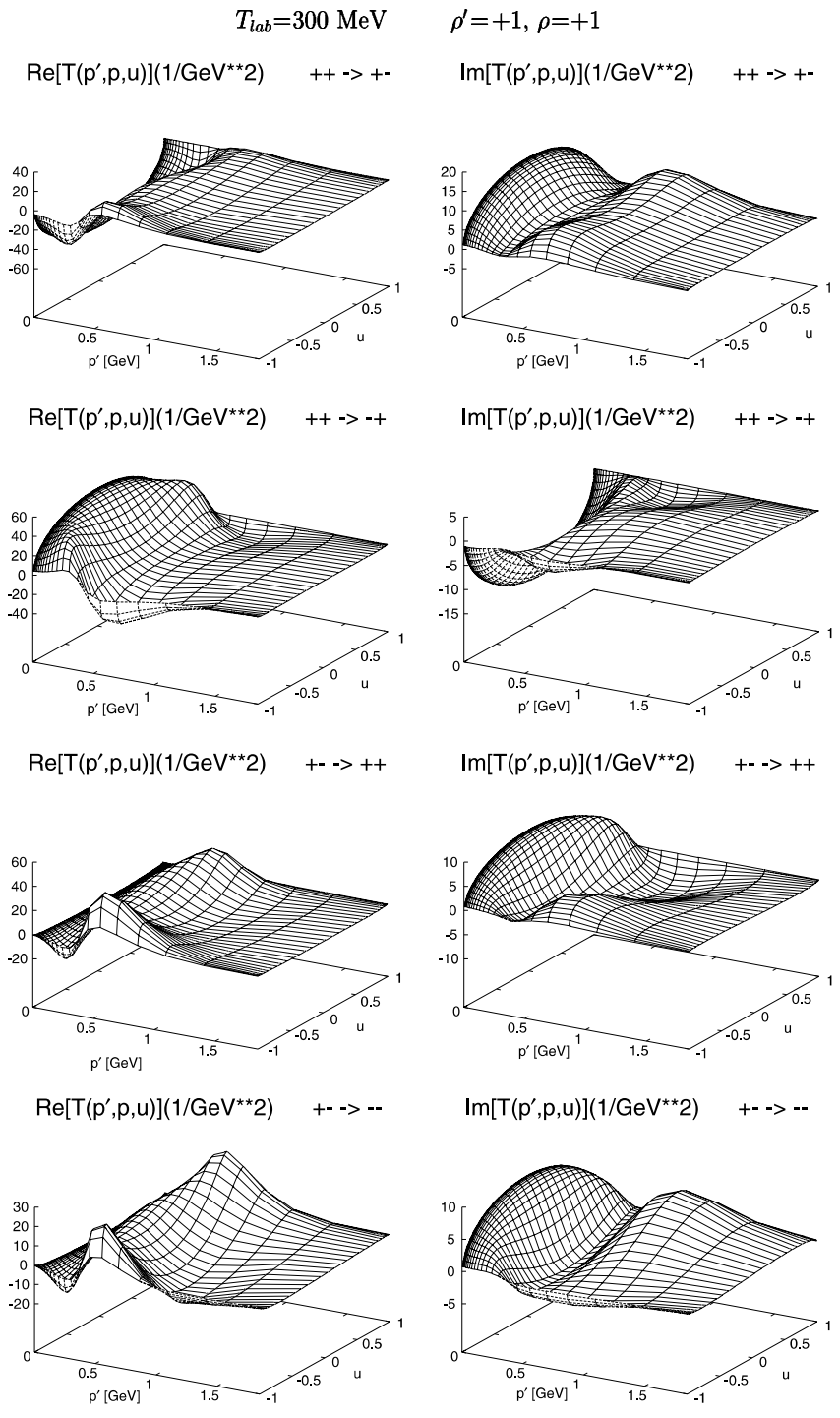

Fig. 7. Off-mass-shell amplitudes for the *np* process with $\rho = +1, \rho' = +1$

as the $\rho' = +1$ amplitudes. Therefore, degrees of freedom corresponding to negative-energy states have considerable weight in the covariant spectator formalism.

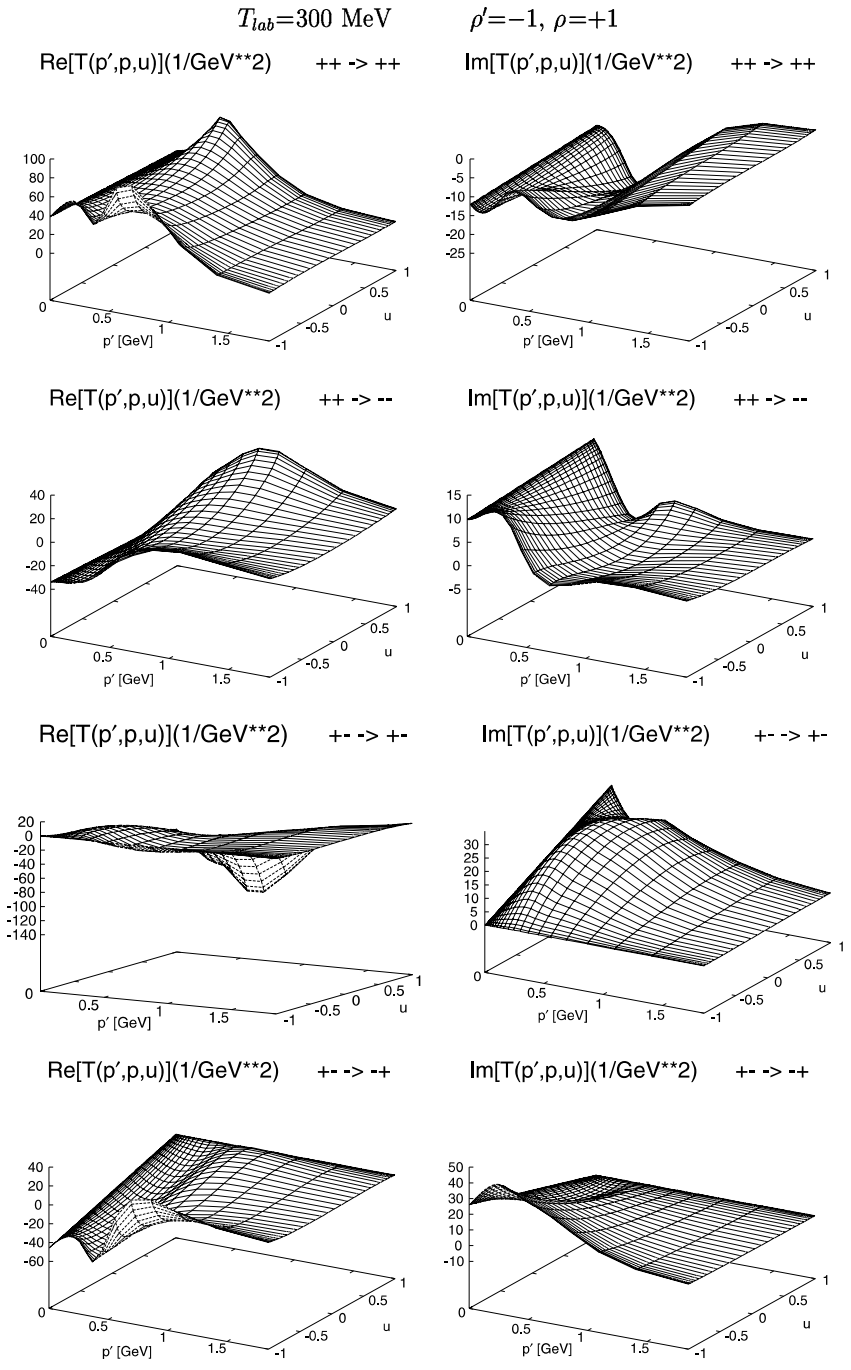

Fig. 8. Off-mass-shell amplitudes for the *np* process with $\rho = +1, \rho' = -1$

4.3 Breaking of PWD for High Energies

We present here the study of the PWD convergence as a function of the energy. To perform this decomposition we follow ref. [24]. Fig. 10 shows the convergence of the PWD to the full calculation for a particular neutron-proton on-mass-shell T

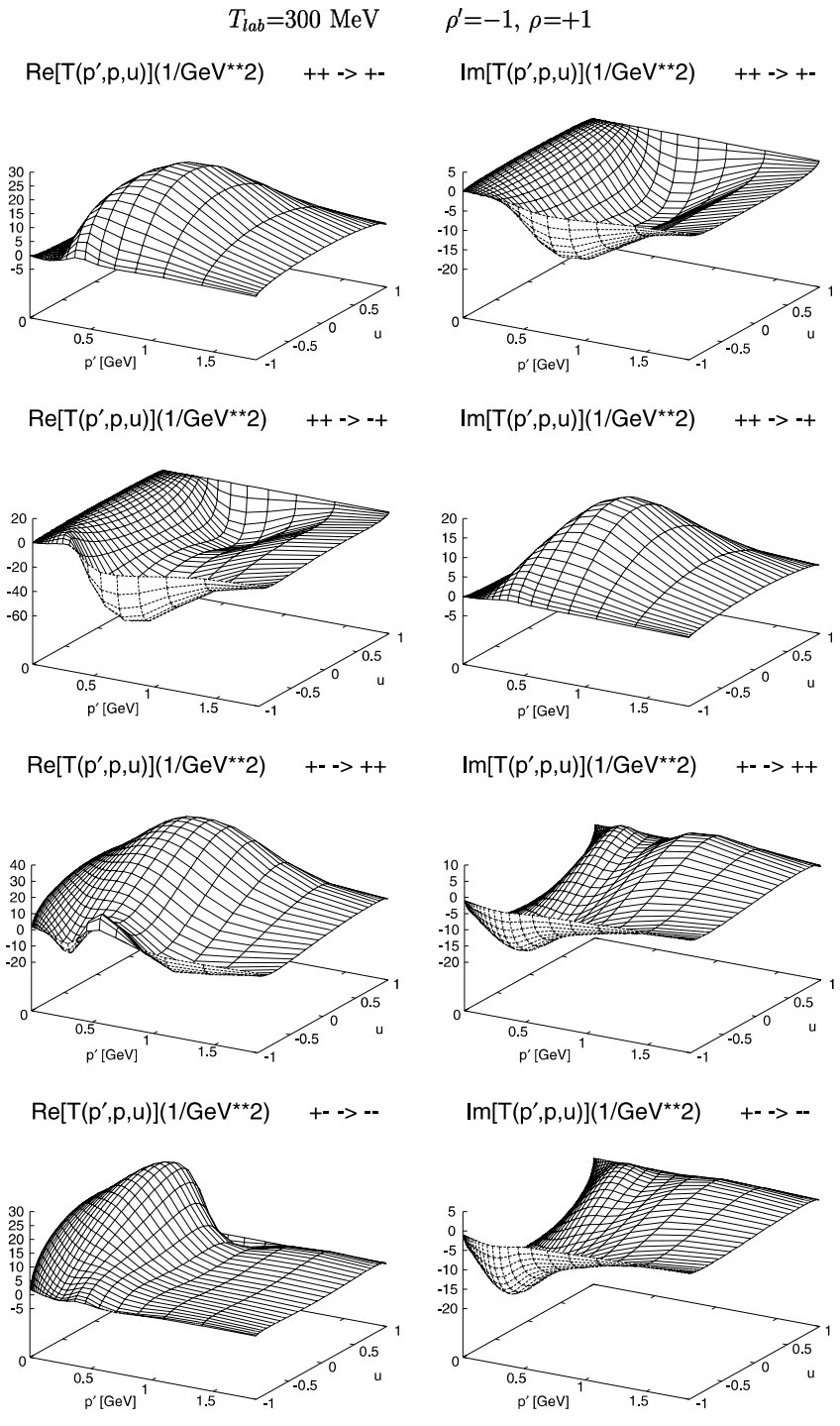

Fig. 9. Off-mass-shell amplitudes for the *np* process with $\rho = +1, \rho' = -1$

matrix, for three energy cases. We notice here that the imaginary part of T converges faster than the real part. For each energy case the criterion for convergence was defined as a deviation less than 1% from the full result.

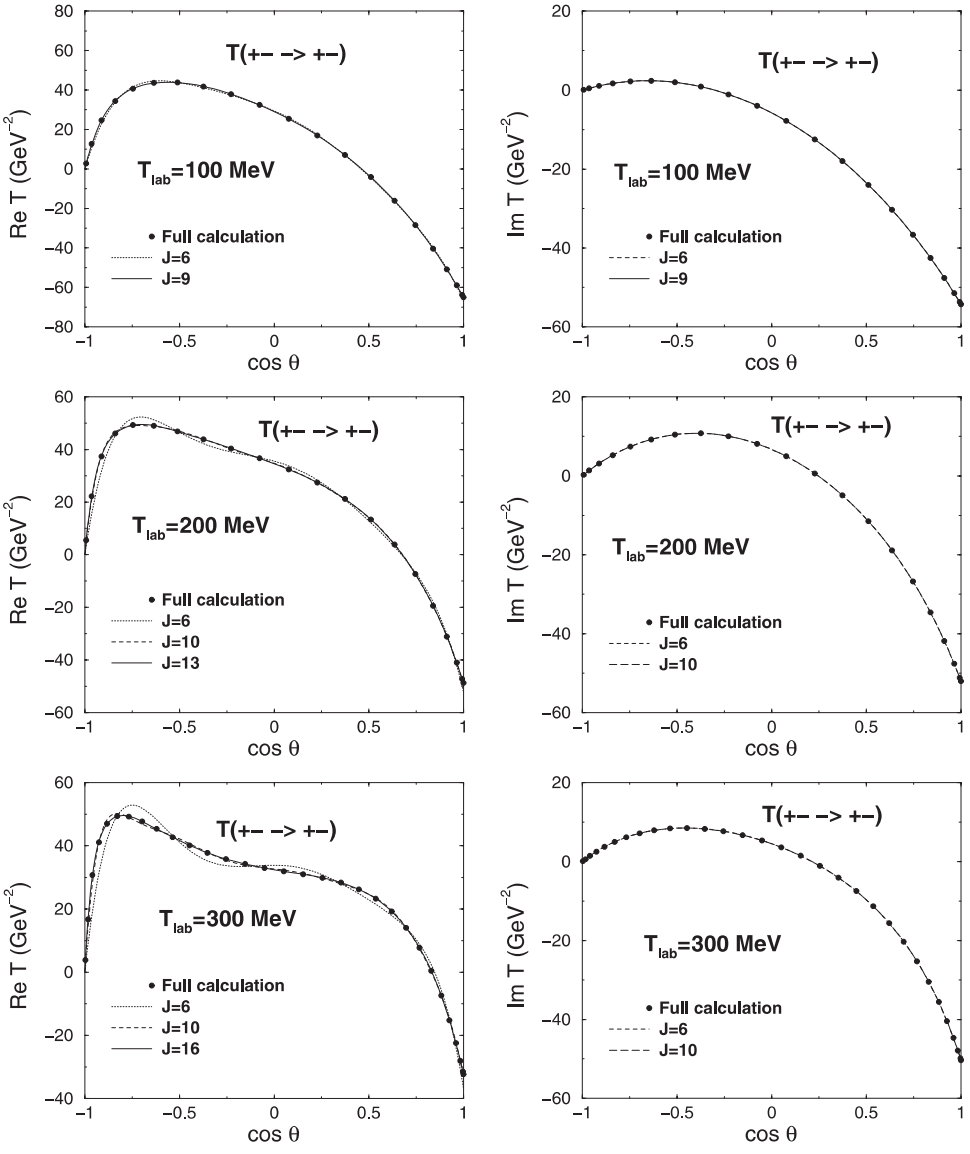

Fig. 10. Partial wave decomposition of the M_3 amplitude for 100, 200, and 300 MeV

The results for 100 MeV shown in Fig. 10 indicate that it is a good approximation at low energies to take $J = 6$ as the highest total angular momentum. This finding is in agreement with the cut-off at $J_{\max} = 6$, corresponding to 24 partial waves, reported in the three-body bound-state relativistic calculations of ref. [16], but an accurate calculation (less than 1%) requires $J_{\max} = 9$.

On the other hand, for 200 MeV we need $J_{\max} = 13$ to achieve convergence. We confirmed also that some helicity channels at 300 MeV require $J_{\max} = 16$, as found in ref. [3], corresponding to 64 partial waves for these amplitudes. Note, however, that not all the helicity amplitudes require the same $J_{\max}$ for convergence (see Figs. 3 and 4). Also, for a given $J_{\max}$ not all the helicity amplitudes correspond to the same number of partial waves. For M_1 and M_2 (which correspond to the

largest number of partial waves) $J_{\max} = 6$, 10, 16 imply 26, 42, and 66 partial waves, respectively. Considering, for instance, the amplitude M_3, plotted in Fig. 10, $J_{\max} = 6$, 10, 16 corresponds to 24, 40, and 64 partial waves, respectively. As mentioned before, this large number of partial waves makes the PWD method impracticable to generate the two-body amplitudes required as an input for the three-body bound or scattering calculations [4].

We also stress that the number of partial waves needed for convergence of the off-mass-shell amplitudes is in general larger than the number required for the on-mass-shell amplitudes: As it was shown by ref. [8], the number of partial waves involved in the bound-state problem of the three-particle system, for the off-shell momentum of the order of a few MeV/c, can be quite large, even for a scalar potential. Finally we report that with a realistic model, which includes pion exchange, the number of partial waves to converge for the on-mass-shell amplitudes is even larger than for the scalar case. More precisely, if the pion is not included in the kernel at 300 MeV, we verified that one needs only $J_{\max} = 6$. That means that, as expected, the long range of the pion exchange is responsible for increasing $J_{\max}$ from 6 to 16.

5 Conclusions

We considered the spectator equation for nucleons. Its solution depends on the helicities of the particles, as well as on their ρ-spins ($\rho' = +1$ for the positive-energy state component and $\rho' = -1$ for the negative-energy state component).

After an analytical integration over the azimuthal variable φ, the scattering amplitude is solved without partial wave decomposition using the Padé method. This method revealed to be efficient and suitable for the solution of the relativistic integral equation without partial wave decomposition. For $T_{\mathrm{lab}} < 320$ MeV, 11 to 15 Padé terms were needed for convergence, depending on the helicity case.

Strong form factors and a prescription for the exchange kernel different from the ones considered in other calculations within the spectator formalism are used. When both particles are on-mass-shell the present prescription for the exchange kernel gives rise to the kernel directly obtained from the Feynman rules. This is important in view of possible applications to problems where the fields are not effective, the $q\bar{q}$ bound state and the quark-exchange diagrams in $\pi\pi$ scattering.

We fitted an OBE interaction to the *np* differential cross section in the energy range of 100–320 MeV. We let the percentage of PS and PV admixture floating as a free parameter in the fit, and it turned out that the PV coupling was favored by the fit, which is in agreement with arguments of chiral symmetry.

We studied the convergence of the PWD method as a function of the energy. We concluded that above $T_{\mathrm{lab}} = 300$ MeV at least 64 partial waves have to be included for some helicity cases. This large number of terms indicates the breaking down of the PWD method at higher energies for applications in heavier nuclei ($A \geq 3$).

Beyond the $\rho' = +1$ amplitudes involved in the cross-section calculation, we have also calculated the $\rho' = -1$ amplitudes related to processes involving one off-mass-shell particle. These amplitudes are numerically significant in the spectator

formalism and may be used in the calculation of meson-production cross sections [31, 32] and of the $^3\mathrm{He}(e,e')\mathrm{X}$-reaction observables for 1–10 GeV energies [1].

While we consider here the particular case of the relativistic spectator equation, the method can be extended to other quasi-potential equations. Besides, it is efficient and not CPU-time expensive, avoids the problem of the very large number of partial waves needed in PWD methods for the *NN* off-mass-shell amplitudes, does not have the numerical instability of the large orbital angular PWD results (due to oscillations of the Legendre polynomials) [8], and finally, it determines the helicity or polarized amplitudes directly, without additional numerical recombination or decomposition.

Acknowledgements. This work was performed partially under grant PRAXIS XXI BD/9450/96 and grant POCT/FNU/50358/2002. One of the authors (G.R.) would like to thank Alfred Stadler for helpful discussions. M.T.P. and G.R. thank Franz Gross and Charlotte Elster for discussions, and the Jefferson Laboratory Theory group for the hospitality during their visit.

Appendix A. States of Helicities

A.1 Positive-Energy State Spinors (u_j^+)

Following refs. [33, 34], we use the definitions for the spinors of particle 1 (momentum k_1) and 2 (momentum k_2),

$$u(k_j,\lambda) = N_k \begin{bmatrix} 1 \\ \lambda\tilde{k} \end{bmatrix} |\lambda\rangle_j \qquad (j=1,2), \tag{A.1}$$

with the normalization

$$N_k = \sqrt{\frac{m+E_{\mathbf{k}}}{2m}}, \tag{A.2}$$

$$\tilde{k} = \frac{\mathrm{k}}{m+E_{\mathbf{k}}}. \tag{A.3}$$

Note that the spinors depend only on the three-momentum.

The Pauli spinors of particles 1 and 2,

$$|\lambda\rangle_1 = \chi_\lambda(\hat{\mathbf{k}}), \tag{A.4}$$

$$|\lambda\rangle_2 = \psi_\lambda(\hat{\mathbf{k}}), \tag{A.5}$$

are related by

$$\psi_\lambda(\hat{\mathbf{k}}) = \chi_{-\lambda}(\hat{\mathbf{k}}). \tag{A.6}$$

Initial- and final-state Pauli spinors are presented in Table A.1.

A.2 Negative-Energy Spinor States (u_j^-)

The negative-energy spinors are constructed from positive-energy states using the charge-conjugation operator C [6, 33, 34],

$$v(k_1,\lambda) = (-1)\lambda C\bar{u}^T(k_2,\lambda), \tag{A.7}$$

$$v(k_2,\lambda) = \lambda C\bar{u}_1^T(k_1,\lambda), \tag{A.8}$$

Table A.1. Pauli helicity states. The phase differences between these spinors and the ones of refs. [33, 34] are due to the fact that we consider, for convenience, the convention of rotations of ref. [34] and the phase convention for particle 2 of ref. [33]

	Initial state	
	$\lambda = 1$	$\lambda = -1$
$\chi_\lambda(\hat{\mathbf{z}})$	$\begin{pmatrix} 1 \\ 0 \end{pmatrix}$	$\begin{pmatrix} 0 \\ 1 \end{pmatrix}$
$\psi_\lambda(\hat{\mathbf{z}})$	$\begin{pmatrix} 0 \\ 1 \end{pmatrix}$	$\begin{pmatrix} 1 \\ 0 \end{pmatrix}$
	Final state	
	$\lambda' = 1$	$\lambda' = -1$
$\chi'_{\lambda'}(\theta,\varphi)$	$\begin{pmatrix} \cos\frac{\theta}{2}\exp\left[-i\frac{\varphi}{2}\right] \\ \sin\frac{\theta}{2}\exp\left[i\frac{\varphi}{2}\right] \end{pmatrix}$	$\begin{pmatrix} -\sin\frac{\theta}{2}\exp\left[-i\frac{\varphi}{2}\right] \\ \cos\frac{\theta}{2}\exp\left[i\frac{\varphi}{2}\right] \end{pmatrix}$
$\psi'_{\lambda'}(\theta,\varphi)$	$\begin{pmatrix} -\sin\frac{\theta}{2}\exp\left[-i\frac{\varphi}{2}\right] \\ \cos\frac{\theta}{2}\exp\left[i\frac{\varphi}{2}\right] \end{pmatrix}$	$\begin{pmatrix} \cos\frac{\theta}{2}\exp\left[-i\frac{\varphi}{2}\right] \\ \sin\frac{\theta}{2}\exp\left[i\frac{\varphi}{2}\right] \end{pmatrix}$

where $C = -i\gamma^0\gamma^2$ and T indicates matrix transposition. The relative factors are introduced by convenience. As a result we get

$$v(k_j,\lambda) = N_k \begin{bmatrix} -\lambda\tilde{\boldsymbol{k}} \\ 1 \end{bmatrix} |\lambda\rangle_j. \tag{A.9}$$

Appendix B. Kernel $\bar{\mathcal{V}}$

In this appendix we describe the analytical structure of the OBE kernel. As mentioned before, for any isospin state I, the kernel $\bar{\mathcal{V}}$ contains the direct $\mathcal{V}$ term and the exchange-kernel $\widehat{\mathcal{V}}$ term,

$$\bar{\mathcal{V}}^{+\rho',+\rho}_{\lambda'_1\lambda'_2,\lambda_1\lambda_2}(p',k;P) = \mathcal{V}^{+\rho',+\rho}_{\lambda'_1\lambda'_2,\lambda_1\lambda_2}(p',k;P) + (-1)^I \widehat{\mathcal{V}}^{+\rho',+\rho}_{\lambda'_1\lambda'_2,\lambda_1\lambda_2}(p',k;P). \tag{B.1}$$

The kernel function includes 2 vertex form factors defined by Eq. (3.32). As discussed in the text, one nucleon is always on-mass-shell and therefore the corresponding form factor reduces simply to 1. In the OBE-potential matrix element the product of the 2 vertex form factors reads then

$$F_i(p'_1,k_1)F_i(p'_2,k_2) = [f_{m_i}(q^2)]^2 f_N(p'^2_2) f_N(k_2^2). \tag{B.2}$$

Only the off-mass-shell nucleon is modified by the inclusion of the nucleon form factor. The off-mass-shell nucleon with momentum $k_2 = (W - E_{\mathbf{k}}, -\mathbf{k})$ enters the exchange diagram with the factor

$$f_N(k_2^2) = \left[\frac{\tilde{\Lambda}_N^2}{\tilde{\Lambda}_N^2 + W^2(W-2E_{\mathbf{k}})^2}\right]^2. \tag{B.3}$$

For meson i the potential direct term is given by

$$\begin{aligned}\mathcal{V}^{+\rho',+\rho}_{\lambda'_1\lambda'_2,\lambda_1\lambda_2}(p',k;P) = \delta_I \frac{g_i^2}{\mu_i^2 - q^2} &\bar{\boldsymbol{u}}^+(p'_1,\lambda'_1)\Lambda_1(p'_1,k_1)u^+(k_1,\lambda_1) \\ &\times \bar{\boldsymbol{u}}^{\rho'}(p'_2,\lambda'_2)\Lambda_2(p'_2,k_2)u^{\rho}(k_2,\lambda_2)[f_{m_i}(q^2)]^2 f_N(p'^2_2) f_N(k_2^2),\end{aligned} \tag{B.4}$$

where Λ_j ($j = 1, 2$) is the vertex operator for the mesons π, σ, ρ, and ω, and the exchange momentum is

$$q^2 = (E_{\mathbf{p}'} - E_{\mathbf{k}})^2 - (\mathbf{p}' - \mathbf{k})^2. \tag{B.5}$$

The πNN vertex is defined by Eq. (2.8). For the other mesons we take the definitions of ref. [6] (with $\lambda_v = 1$).

For vector mesons we make the substitution

$$\Lambda_1\Lambda_2 \to \Lambda_1^{\mu}(p_1', k_1)\Lambda_2^{\nu}(p_2', k_2)\left[g_{\mu\nu} + \frac{(p_1' - k_1)_{\mu}(p_2' - k_2)_{\nu}}{\mu_i^2}\right]. \tag{B.6}$$

Similarly, for the exchange term of the potential we have

$$\begin{aligned}\widehat{\mathcal{V}}^{+\rho',+\rho}_{\lambda_1'\lambda_2',\lambda_1\lambda_2}(p', k; P) = \delta_I \frac{g_i^2}{\mu_i^2 - \hat{q}^2}\bar{u}^{+}(p_1', \lambda_1')\Lambda_1(p_1', k_2)u^{\rho}(k_2, \lambda_2) \\ \times \bar{u}^{\rho'}(p_2', \lambda_2')\Lambda_2(p_2', k_1)u^{+}(k_1, \lambda_1)[f_{m_i}(\hat{q}^2)]^2 f_N(p_2'^2) f_N(k_2^2),\end{aligned} \tag{B.7}$$

where, according to the *on-mass-shell prescription* (see Sect. 3.3), the exchange momentum is

$$\hat{q}^2 = (E_{\mathbf{p}'} - E_{\mathbf{k}})^2 - (\mathbf{p}' + \mathbf{k})^2. \tag{B.8}$$

For vector mesons the replacement is now

$$\Lambda_1\Lambda_2 \to \Lambda_1^{\mu}(p_1', k_2)\Lambda_2^{\nu}(p_2', k_1)\left[g_{\mu\nu} + \frac{(p_1' - k_2)_{\mu}(p_2' - k_1)_{\nu}}{\mu_i^2}\right]. \tag{B.9}$$

To evaluate the contributions of all mesons we decompose the vertex projections on the asymptotic states in terms of amplitudes that involve only on-mass-shell couplings and amplitudes with off-mass-shell corrections. We evaluate those expressions as matrix elements between the asymptotic states $u_1^{\pm}(p, \lambda_1)$ and $u_2^{\pm}(p, \lambda_2)$. Finally, we write all results in terms of coefficients to be defined in the next sections. The formulas presented in Sect. B.1 are for the direct term and in Sect. B.2 for the exchange term.

B.1 Direct Kernel

We will write the direct kernel in terms of the following variables,

$$Q_j^{\pm} = \lambda_j'\tilde{\mathbf{p}}' \pm \lambda_j\tilde{\mathbf{k}}, \tag{B.10}$$

$$R_j^{\pm} = \lambda_j'\tilde{\mathbf{p}}'\lambda_j\tilde{\mathbf{k}} \pm 1 \tag{B.11}$$

($j = 1, 2$, $\tilde{k}$ comes from the definition of spinors, see Appendix A), and the following auxiliary functions

$$Z_1^0(\hat{\mathbf{p}}', \hat{\mathbf{k}}) = \chi_{\lambda_1'}'^{\dagger}(\hat{\mathbf{p}}')\chi_{\lambda_1}(\hat{\mathbf{k}}), \tag{B.12}$$

$$Z_2^0(\hat{\mathbf{p}}', \hat{\mathbf{k}}) = \psi_{\lambda_2'}'^{\dagger}(\hat{\mathbf{p}}')\psi_{\lambda_2}(\hat{\mathbf{k}}), \tag{B.13}$$

$$Z_1^i(\hat{\mathbf{p}}', \hat{\mathbf{k}}) = \chi_{\lambda_1'}'^{\dagger}(\hat{\mathbf{p}}')\sigma_i^{(1)}\chi_{\lambda_1}(\hat{\mathbf{k}}), \tag{B.14}$$

$$Z_2^i(\hat{\mathbf{p}}', \hat{\mathbf{k}}) = \psi_{\lambda_2'}'^{\dagger}(\hat{\mathbf{p}}')\sigma_i^{(2)}\psi_{\lambda_2}(\hat{\mathbf{k}}). \tag{B.15}$$

The Z_j^{α} functions ($j = 1, 2$, $\alpha = 0, \ldots, 3$) are calculated from the Pauli spinors presented in Appendix A. For simplicity sometimes we suppress the arguments of Z_j^{α}.

B.1.1 σ Exchange

$$\begin{aligned}\mathcal{V}^{+\rho',+\rho}_{\lambda_1'\lambda_2',\lambda_1\lambda_2}(p', k) = -\frac{g_{\sigma}^2}{\mu_{\sigma}^2 - q^2}[f_{\sigma}(q^2)]^2 f_N(p_2'^2) f_N(k_2^2) \\ \times N_{p'}^2 N_k^2\, H_{\sigma}(p', k)\, Z_1^0(\hat{\mathbf{p}}', \hat{\mathbf{k}}) Z_2^0(\hat{\mathbf{p}}', \hat{\mathbf{k}}).\end{aligned} \tag{B.16}$$

$H_\sigma(p',k)$ is also a function of the helicity ρ-states given by

$$H_\sigma(p',k) = A(p',k)B^{\rho'\rho}(p',k), \tag{B.17}$$

where

$$\begin{aligned} A(p',k) &= -R_1^-, \\ B^{++}(p',k) &= -R_2^-, \\ B^{+-}(p',k) &= -Q_2^+, \\ B^{-+}(p',k) &= -Q_2^+, \\ B^{--}(p',k) &= R_2^-. \end{aligned}$$

For large k we have $H_\sigma(p',k) \sim 1$.

B.1.2 π Exchange

$$\begin{aligned} \mathcal{V}^{+\rho',+\rho}_{\lambda_1'\lambda_2',\lambda_1\lambda_2}(p',k;P) = \delta_I \frac{g_\pi^2}{\mu_\pi^2 - q^2}[f_\pi(q^2)]^2 f_N(p_2'^2) f_N(k_2^2) \\ \times N_{p'}^2 N_k^2 H_\pi(p',k) Z_1^0(\hat{\mathbf{p}}',\hat{\mathbf{k}}) Z_2^0(\hat{\mathbf{p}}',\hat{\mathbf{k}}). \end{aligned} \tag{B.18}$$

$H_\pi(p',k)$ is also a function of the helicity ρ-states. We can write it as

$$H_\pi(p',k) = A(p',k)B^{\rho'\rho}(p',k), \tag{B.19}$$

where

$$\begin{aligned} A(p',k) &= -Q_1^-, \\ B^{++}(p',k) &= -Q_2^- - (1-\lambda)\frac{E_{\mathbf{p}'} - E_{\mathbf{k}}}{m} Q_2^+, \\ B^{+-}(p',k) &= \lambda R_2^+ + (1-\lambda)\frac{E_{\mathbf{p}'} - E_{\mathbf{k}}}{m} R_2^-, \\ B^{-+}(p',k) &= -\lambda R_2^+ + (1-\lambda)\frac{E_{\mathbf{p}'} - E_{\mathbf{k}}}{m} R_2^-, \\ B^{--}(p',k) &= (1-2\lambda)Q_2^- + (1-\lambda)\frac{E_{\mathbf{p}'} - E_{\mathbf{k}}}{m} Q_2^+. \end{aligned}$$

For large k we have $H_\pi(p',k) \sim 1$ for PS coupling, and $H_\pi(p',k) \sim \mathrm{k}/m$ for PV coupling.

B.1.3 Vector Meson Exchange

$$\mathcal{V}^{+\rho',+\rho}_{\lambda_1'\lambda_2',\lambda_1\lambda_2}(p',k;P) = \delta_I \frac{g_v^2}{\mu_v^2 - q^2}[f_v(q^2)]^2 f_N(p_2'^2) f_N(k_2^2) N_{p'}^2 N_k^2 H_v(p',k), \tag{B.20}$$

$$\begin{aligned} H_v(p',k) = r_0 Z_1^0 Z_2^0 + r_1 \sum_{i=1}^3 Z_1^i Z_2^i + r_2 \sum_{i=1}^3 (\mathrm{p}_i' + \mathrm{k}_i) Z_1^0 Z_2^i \\ + r_3 \sum_{i=1}^3 (\mathrm{p}_i' + \mathrm{k}_i) Z_1^i Z_2^0 + r_4 \sum_{i=1}^3 (\mathrm{p}_i' + \mathrm{k}_i)^2 Z_1^0 Z_2^0. \end{aligned} \tag{B.21}$$

The coefficients r_l ($l = 0, \ldots, 4$) are functions of the momenta and the helicity ρ-states. They can be written explicitly as

$$\begin{aligned} r_0 &= [\bar{a}_1\alpha_1 + \bar{b}_1\alpha_3(E_{\mathbf{p}'} + E_{\mathbf{k}})][\bar{a}_2\beta_1 + \bar{b}_2\beta_3(E_{\mathbf{p}'} + E_{\mathbf{k}})], \\ r_1 &= \bar{a}_1\alpha_2(\bar{a}_2\beta_2 + \bar{c}_2\beta_4), \\ r_2 &= \bar{a}_1\alpha_2\bar{b}_2\beta_3, \\ r_3 &= \bar{b}_1\alpha_3(\bar{a}_2\beta_2 + \bar{c}_2\beta_4), \\ r_4 &= \bar{b}_1\alpha_3\bar{b}_2\beta_3, \end{aligned}$$

where

$$\bar{a}_1 = 1 + \kappa_v,$$
$$\bar{b}_1 = -\frac{\kappa_v}{2m},$$
$$\bar{a}_2 = 1 + \rho'\kappa_v\delta_{\rho'\rho},$$
$$\bar{b}_2 = -\frac{\kappa_v}{2m},$$
$$\bar{c}_2 = -\kappa_v\frac{E_{\mathbf{p}'} - E_{\mathbf{k}}}{m}.$$

The coefficients α are related to the helicity states of particle 1 (on-mass-shell nucleon)

$$\alpha_1 = R_1^+,$$
$$\alpha_2 = Q_1^+,$$
$$\alpha_3 = -R_1^-.$$

The coefficients β are related to particle 2. They depend on helicity ρ-states according to the table:

	$++$	$+-$	$-+$	$--$
β_1	R_2^+	Q_2^-	$-Q_2^-$	R_2^+
β_2	Q_2^+	$-R_2^-$	$-R_2^-$	$-Q_2^+$
β_3	$-R_2^-$	$-Q_2^+$	$-Q_2^+$	R_2^-
β_4	$-Q_2^-$	R_2^+	$-R_2^+$	$-Q_2^-$

For large k we have $H_v(p',k) \sim 1$ when $\kappa_v = 0$; $H_v(k,k) \sim \mathrm{k}^2/m^2$ and $H_v(p',k) \sim \mathrm{k}/m$ when $\kappa_v \neq 0$.

B.2 Exchange Kernel

For the exchange term we introduce the auxiliary variables

$$\widehat{Q}_1^{\pm} = \lambda_1'\tilde{p}' \pm \lambda_2\tilde{k}, \tag{B.22}$$
$$\widehat{Q}_2^{\pm} = \lambda_2'\tilde{p}' \pm \lambda_1\tilde{k}, \tag{B.23}$$
$$\widehat{R}_1^{\pm} = \lambda_1'\tilde{p}'\lambda_1\tilde{k} \pm 1, \tag{B.24}$$
$$\widehat{R}_2^{\pm} = \lambda_2'\tilde{p}'\lambda_1\tilde{k} \pm 1 \tag{B.25}$$

(resulting from the analogue variables defined for the direct kernel with the replacement $\lambda_1 \rightleftharpoons \lambda_2$) and the auxiliary functions

$$\widehat{Z}_1^0(\hat{\mathbf{p}}',\hat{\mathbf{k}}) = \chi_{\lambda_1'}'^{\dagger}(\hat{\mathbf{p}}')\psi_{\lambda_2}(\hat{\mathbf{k}}), \tag{B.26}$$
$$\widehat{Z}_2^0(\hat{\mathbf{p}}',\hat{\mathbf{k}}) = \psi_{\lambda_1'}'^{\dagger}(\hat{\mathbf{p}}')\chi_{\lambda_1}(\hat{\mathbf{k}}), \tag{B.27}$$
$$\widehat{Z}_1^i(\hat{\mathbf{p}}',\hat{\mathbf{k}}) = \chi_{\lambda_1'}'^{\dagger}(\hat{\mathbf{p}}')\sigma_i^{(1)}\psi_{\lambda_2}(\hat{\mathbf{k}}), \tag{B.28}$$
$$\widehat{Z}_2^i(\hat{\mathbf{p}}',\hat{\mathbf{k}}) = \psi_{\lambda_2'}'^{\dagger}(\hat{\mathbf{p}}')\sigma_i^{(2)}\chi_{\lambda_1}(\hat{\mathbf{k}}). \tag{B.29}$$

These functions are to be evaluated as matrix elements between Pauli spinors.

B.2.1 σ Exchange

$$\widehat{\mathcal{V}}^{+\rho',+\rho}_{\lambda_1'\lambda_2',\lambda_1\lambda_2}(p',k;P) = -\frac{g_\sigma^2}{\mu_\sigma^2 - \hat{q}^2}[f_\sigma(\hat{q}^2)]^2 f_N(p_2'^2) f_N(k_2^2) \times N_{p'}^2 N_k^2 \widehat{H}_\sigma(p',k)\widehat{Z}_1^0(\hat{\mathbf{p}}',\hat{\mathbf{k}})\widehat{Z}_2^0(\hat{\mathbf{p}}',\hat{\mathbf{k}}), \tag{B.30}$$
$$\widehat{H}_\sigma(p',k) = A^{\rho'}(p',k)B^{\rho}(p',k), \tag{B.31}$$

where

$$A^+(p',k) = -\widehat{R}_1^-,$$
$$A^-(p',k) = -\widehat{Q}_1^+,$$
$$B^+(p',k) = -\widehat{R}_2^-,$$
$$B^-(p',k) = -\widehat{Q}_2^+.$$

For large k we have $\widehat{H}_\sigma(p',k) \sim 1$.

B.2.2 π Exchange

$$\widehat{\mathcal{V}}^{+\rho',+\rho}_{\lambda_1'\lambda_2',\lambda_1\lambda_2}(p',k;P) = \delta_I \frac{g_\pi^2}{\mu_\pi^2 - q^2}[f_\pi(q^2)]^2 f_N(p_2'^2) f_N(k_2^2) \times N_{p'}^2 N_k^2 \widehat{H}_\pi(p',k)\widehat{Z}_1^0(\hat{\mathbf{p}}',\hat{\mathbf{k}})\widehat{Z}_2^0(\hat{\mathbf{p}}',\hat{\mathbf{k}}), \tag{B.32}$$

$$\widehat{H}_\pi(p',k) = A^{\rho'}(p',k)B^{\rho}(p',k), \tag{B.33}$$

where

$$A^+(p',k) = -\widehat{Q}_1^- - (1-\lambda)\frac{W - 2E_{\mathbf{k}}}{2m}\widehat{Q}_1^+,$$

$$A^-(p',k) = \lambda\widehat{R}_1^+ + (1-\lambda)\frac{W - 2E_{\mathbf{k}}}{2m}\widehat{R}_1^-,$$

$$B^+(p',k) = -\widehat{Q}_2^- + (1-\lambda)\frac{W - 2E_{\mathbf{p}'}}{2m}\widehat{Q}_2^+,$$

$$B^-(p',k) = -\lambda\widehat{R}_2^+ - (1-\lambda)\frac{W - 2E_{\mathbf{p}'}}{2m}\widehat{R}_2^-.$$

For large k we have $\widehat{H}_\pi(p',k) \sim 1$ for PS coupling, $\widehat{H}_\pi(p',k) \sim \mathrm{k}/m$ and $\widehat{H}_\pi(k,k) \sim \mathrm{k}^2/m^2$ for PV coupling.

B.2.3 Vector Meson Exchange

$$\widehat{\mathcal{V}}^{+\rho',+\rho}_{\lambda_1'\lambda_2',\lambda_1\lambda_2}(p',k;P) = \delta_I \frac{g_v^2}{\mu_v^2 - q^2}[f_v(q^2)]^2 f_N(p_2'^2) f_N(k_2^2) N_{p'}^2 N_k^2 \widehat{H}_v(p',k), \tag{B.34}$$

$$\widehat{H}_v(p',k) = (r_0 + r_5)\widehat{Z}_1^0\widehat{Z}_2^0 + r_1\sum_{i=1}^3 \widehat{Z}_1^i\widehat{Z}_2^i + r_2\sum_{i=1}^3(\mathrm{p}_i' - \mathrm{k}_i)\widehat{Z}_1^0\widehat{Z}_2^i + r_3\sum_{i=1}^3(\mathrm{p}_i' - \mathrm{k}_i)\widehat{Z}_1^i\widehat{Z}_2^0 + r_4\sum_{i=1}^3(\mathrm{p}_i' - \mathrm{k}_i)^2\widehat{Z}_1^0\widehat{Z}_2^0. \tag{B.35}$$

The coefficients r_l ($l = 0,\ldots,4$) are functions of the momenta p′, k and helicity ρ-states. Explicitly we have

$$r_0 = [\bar{a}_1\alpha_1 + \bar{b}_1\alpha_3(E_{\mathbf{p}'} + E_{\mathbf{k}})][\bar{a}_2\beta_1 + \bar{b}_2\beta_3(E_{\mathbf{p}'} + E_{\mathbf{k}})],$$
$$r_1 = (\bar{a}_1\alpha_2 + \bar{c}_1\alpha_4)(\bar{a}_2\beta_2 + \bar{c}_2\beta_4),$$
$$r_2 = (\bar{a}_1\alpha_2 + \bar{c}_1\alpha_4)\bar{b}_2\beta_3,$$
$$r_3 = \bar{b}_1\alpha_3(\bar{a}_2\beta_2 + \bar{c}_2\beta_4),$$
$$r_4 = \bar{b}_1\alpha_3\bar{b}_2\beta_3,$$
$$r_5 = \frac{\alpha_5\beta_5}{\mu^2}.$$

The r_l coefficients for the exchange kernel are not related to the direct kernel coefficients. The inclusion of r_5 results from Eq. (B.9) when the same particle is not on-mass-shell in both the initial and final states. In this case we have

$$\bar{a}_1 = 1 + \kappa_v \delta_{\rho +},$$
$$\bar{b}_1 = -\frac{\kappa_v}{2m},$$
$$\bar{c}_1 = -\kappa_v \frac{W - 2E_{\mathbf{k}}}{2m},$$
$$\bar{a}_2 = 1 + \kappa_v \delta_{\rho' +},$$
$$\bar{b}_2 = -\frac{\kappa_v}{2m},$$
$$\bar{c}_2 = \kappa_v \frac{W - 2E_{\mathbf{p}'}}{2m}.$$

The coefficients α depend on λ_1', λ_2, and ρ. The coefficients β are functions of λ_2', λ_1, and ρ'. The results are presented in the following table:

ρ	$+$	$-$
α_1	$\widehat{R}_1^+$	$\widehat{Q}_1^-$
α_2	$\widehat{Q}_1^+$	$-\widehat{R}_1^-$
α_3	$-\widehat{R}_1^-$	$-\widehat{Q}_1^+$
α_4	$-\widehat{Q}_1^-$	$\widehat{R}_1^+$
α_5	$(2E_{\mathbf{k}} - W)\widehat{R}_1^+$	$(2E_{\mathbf{k}} - W)\widehat{Q}_1^- - 2m\widehat{Q}_1^+$
ρ'	$+$	$-$
β_1	$\widehat{R}_2^+$	$-\widehat{Q}_2^-$
β_2	$\widehat{Q}_2^+$	$-\widehat{R}_2^-$
β_3	$-\widehat{R}_2^-$	$-\widehat{Q}_2^+$
β_4	$-\widehat{Q}_2^-$	$-\widehat{R}_2^+$
β_5	$(W - 2E_{\mathbf{p}'})\widehat{R}_2^+$	$-(W - 2E_{\mathbf{p}'})\widehat{Q}_2^- + 2m\widehat{Q}_2^+$

For large k we have $\widehat{H}_v(p', k) \sim 1$ when $\kappa_v = 0$; $\widehat{H}_v(k, k) \sim \mathrm{k}^2/m^2$ and $\widehat{H}_v(p', k) \sim \mathrm{k}/m$ when $\kappa_v \neq 0$.

B.3 α and β Coefficients

The coefficients α and β are derived from the formulas listed below, where we use $u_1' = u^+(p_1', \lambda_1')$, $u_1 = u^+(p_1, \lambda_1)$, $w_2' = u^{\rho'}(p_2', \lambda_2')$, and $w_2 = u^{\rho}(p_2, \lambda_2)$.

B.3.1 Direct Kernel

$$\bar{u}_1' \gamma^0 u_1 = \alpha_1 N_{p'} N_k Z_1^0,$$
$$\bar{u}_1' \gamma^i u_1 = \alpha_1 N_{p'} N_k Z_1^i,$$
$$\bar{u}_1' u_1 = \alpha_3 N_{p'} N_k Z_1^0,$$
$$\bar{w}_2' \gamma^0 w_2 = \beta_1 N_{p'} N_k Z_2^0,$$
$$\bar{w}_2' \gamma^i w_2 = \beta_2 N_{p'} N_k Z_2^i,$$
$$\bar{w}_2' w_2 = \beta_3 N_{p'} N_k Z_1^0,$$
$$\bar{w}_2' \gamma^0 \gamma^i w_2 = \beta_4 N_{p'} N_k Z_2^i.$$

B.3.2 Exchange Kernel

$$\begin{aligned}
\bar{\boldsymbol{u}}_1'\gamma^0 w_2 &= \alpha_1 N_{p'} N_k \widehat{\boldsymbol{Z}}_1^0,\\
\bar{\boldsymbol{u}}_1'\gamma^i w_2 &= \alpha_2 N_{p'} N_k \widehat{\boldsymbol{Z}}_1^i,\\
\bar{\boldsymbol{u}}_1' w_2 &= \alpha_3 N_{p'} N_k \widehat{\boldsymbol{Z}}_1^0,\\
\bar{\boldsymbol{u}}_1'\gamma^0\gamma^i w_2 &= \alpha_4 N_{p'} N_k \widehat{\boldsymbol{Z}}_1^i,\\
\bar{\boldsymbol{w}}_2'\gamma^0 u_1 &= \beta_1 N_{p'} N_k \widehat{\boldsymbol{Z}}_2^0,\\
\bar{\boldsymbol{w}}_2'\gamma^i u_1 &= \beta_2 N_{p'} N_k \widehat{\boldsymbol{Z}}_2^i,\\
\bar{\boldsymbol{w}}_2' u_1 &= \beta_3 N_{p'} N_k \widehat{\boldsymbol{Z}}_2^0,\\
\bar{\boldsymbol{w}}_2'\gamma^0\gamma^i u_1 &= \beta_4 N_{p'} N_k \widehat{\boldsymbol{Z}}_2^i.
\end{aligned}$$

Appendix C. φ Rotated Amplitude

In this appendix we derive the relation between the scattering amplitude on the scattering plane ($\mathbf{p}$ is on the z-axis),

$$\mathcal{M}^{+\rho_2',+\rho_2}_{\lambda_1'\lambda_2',\lambda_1\lambda_2}(\mathrm{p}',\theta',0;\mathrm{p};W),$$

and the scattering amplitude on a rotated plane characterized by φ'-rotation in the z-axis,

$$\mathcal{M}^{+\rho_2',+\rho_2}_{\lambda_1'\lambda_2',\lambda_1\lambda_2}(\mathrm{p}',\theta',\varphi';\mathrm{p};W).$$

Thus, we consider the Lorentz transformation

$$\Lambda = R_{-\varphi',0,0} \tag{C.1}$$

that transforms $\mathbf{p}' = (\mathrm{p}',\theta',\varphi')$ into $\mathbf{p}' = (\mathrm{p}',\theta',0)$.

The correspondence between the spinors before and after this Lorentz transformation is

$$S(\Lambda)u_1^\rho(p,\lambda) = \sum_{\lambda'} D_{\lambda'\lambda}(R_\Lambda)u_1^\rho(\Lambda p,\lambda'), \tag{C.2}$$

$$S(\Lambda)u_2^\rho(p,\lambda) = \sum_{\lambda'} D_{-\lambda',-\lambda}(R_\Lambda)u_2^\rho(\Lambda p,\lambda'), \tag{C.3}$$

where $S(\Lambda)$ is the operator that transforms the u,v-states in the Lorentz transformation Λ and D is the usual $D^{1/2}$ Wigner matrix in terms of the rotation angles. The rotation operators are given by

$$R_\Lambda = H^{-1}_{\Lambda p}\Lambda H_p, \tag{C.4}$$

$$R'_\Lambda = H^{-1}_{\Lambda p'}\Lambda H_{p'}. \tag{C.5}$$

In the last equations H_p is the operator that transforms a four-momentum $(m,\mathbf{0})$ into $p = (E_{\mathbf{p}},\mathbf{p})$. Details can be found in ref. [35]. The operation can always be written in a sequence of a boost (L_p) and a rotation ($R_{\hat{\mathbf{p}}}$),

$$H_p = R_{\hat{\mathbf{p}}}L_p. \tag{C.6}$$

After the Lorentz transformation has been done the following relation between the original and the rotated scattering amplitudes is obtained,

$$\mathcal{M}_{\alpha'\beta',\alpha\beta}(\Lambda p',\Lambda p;\Lambda P) = \sum_{\substack{\alpha_1,\beta_1\\ \alpha_2,\beta_2}} S_{\alpha'\alpha_1}(\Lambda)S_{\beta'\beta_1}(\Lambda)\mathcal{M}_{\alpha_1\beta_1,\alpha_2\beta_2}(p',p;P)S^{-1}_{\alpha_2\alpha}(\Lambda)S^{-1}_{\beta_2\beta}(\Lambda). \tag{C.7}$$

For more details see Appendix B of ref. [6].

Changing Eq. (C.7) to the helicity representation according to Eq. (2.4) and using the operator-rotation properties and the invariance of permutation between boost and rotation operators related to the same axis, we finally conclude that

$$\mathcal{M}^{+\rho_2',+\rho_2}_{\lambda_1'\lambda_2',\lambda_1\lambda_2}(\mathrm{p}',\theta',\varphi';\mathrm{p};W)=\exp\left[\frac{\lambda_1-\lambda_2}{2}\varphi'\right]\mathcal{M}^{+\rho_2',+\rho_2}_{\lambda_1'\lambda_2',\lambda_1\lambda_2}(\mathrm{p}',\theta',0;\mathrm{p};W). \tag{C.8}$$

Appendix D. Function *V*

In this appendix we describe how to evaluate V defined by Eq. (3.6). By performing the φ-integration we get

$$V(\mathrm{p}',\theta',\mathrm{k},\theta;\bar{\lambda},W)=\int_0^{2\pi}e^{i\bar{\lambda}\varphi}\bar{\mathcal{V}}(\varphi)\,d\varphi, \tag{D.1}$$

where we use the simplification

$$\bar{\mathcal{V}}(\varphi)=\bar{\mathcal{V}}^{+\rho_2',+\rho}_{\lambda_1'\lambda_2',\lambda_3\lambda_4}(\mathrm{p}',\theta',0;\mathrm{k},\theta,\varphi;W). \tag{D.2}$$

We note that

$$\bar{\lambda}=\frac{\lambda_1-\lambda_2}{2}, \tag{D.3}$$

so $\bar{\lambda}=0,\ \pm1$ (remember that $\lambda_j=\pm1$).

First, we separate the φ-dependent parts from the independent ones (factorization). Next, we analyze the structure of the resulting functions. We need to consider two different cases: the non-vector meson exchange (σ and π) and the vector meson exchange.

D.1 Factorization of $\bar{\mathcal{V}}(\varphi)$

From the expression $\mathcal{V}$ (see Appendix B) we conclude that

$$\bar{\mathcal{V}}(\varphi)=\delta_I\Lambda_m^4 g_m^2\bar{V}(\varphi)\mathcal{R}, \tag{D.4}$$

where

$$\bar{V}(\varphi)=\frac{[f_m(q^2)]^2}{\Lambda_m^4}\frac{g_m^2}{\mu^2-q^2} \tag{D.5}$$

and

$$\mathcal{R}=N_{p'}^2N_k^2f_N(p'^2)f_N(k^2)\tilde{\boldsymbol{H}}_i(p',k). \tag{D.6}$$

In these equations i is the meson index. Also from Appendix B we have

$$\tilde{\boldsymbol{H}}_i(p',k)=H_i(p',k)Z_1^0Z_2^0 \tag{D.7}$$

for a non-vector meson and

$$\tilde{\boldsymbol{H}}_i(p',k)=H_i(p',k) \tag{D.8}$$

for vector mesons. Note that the parameterization (D.6) is valid for the direct term and for the exchange term if we replace q^2 by $\hat{q}^2$, H_i by $\widehat{\boldsymbol{H}}_i$ (and Z_j^0 by $\widehat{Z}_j^0$ for the non-vector case).

Using the definition (3.1)–(3.3) of the coordinates with $\varphi'=0$ for q^2 and $\hat{q}^2$ we can conclude that

$$\bar{V}(\varphi)=\frac{1}{a-b\cos\varphi}\frac{1}{(c-b\cos\varphi)^2}, \tag{D.9}$$

where

$$a = \mu^2 + \mathrm{p}'^2 + \mathrm{k}^2 \mp 2\mathrm{p}'\mathrm{k}\cos\theta'\cos\theta - q_0^2, \tag{D.10}$$

$$b = \pm 2\mathrm{p}'\mathrm{k}\sin\theta'\sin\theta, \tag{D.11}$$

$$c = \Lambda_m^2 + \mathrm{p}'^2 + \mathrm{k}^2 \mp 2\mathrm{p}'\mathrm{k}\cos\theta'\cos\theta - q_0^2. \tag{D.12}$$

The upper sign should be used in the direct term and the lower sign in the exchange term.

D.2 $\mathcal{R}$ in Terms of φ

The next step is to write $\mathcal{R}$ of Eq. (D.6) in terms of φ. We need to consider two separate cases: the non-vector mesons and the vector mesons.

D.2.1 Non-Vector Mesons

For non-vector mesons we can write

$$\mathcal{R} = f(\mathrm{p}', \mathrm{k}) \cdot Z_1^0 Z_2^0. \tag{D.13}$$

The exact expression of $f(\mathrm{p}', \mathrm{k})$ can be easily deduced from Eq. (D.6). Attending to the $Z_1^0 Z_2^0$ dependence in φ, we conclude that

$$\mathcal{R} = f(\mathrm{p}', \mathrm{k}) \cdot (c_0 + c_1 \exp[-i\lambda_3\varphi] + c_2 \exp[i\lambda_3\varphi]), \tag{D.14}$$

where c_l $(l = 0, \ldots, 2)$ are known coefficients depending on the scattering conditions and on the helicity states. We can write

$$V(\mathrm{p}', \theta', \mathrm{k}, \theta; \bar{\lambda}, W) = \delta_I \Lambda_m^4 g_m^2 f(\mathrm{p}', \mathrm{k})[c_0 \mathcal{F}_0(\bar{\lambda}) + c_1 \mathcal{F}_0(\bar{\lambda} - \lambda_3) + c_2 \mathcal{F}_0(\bar{\lambda} + \lambda_3)], \tag{D.15}$$

where the function $\mathcal{F}_0(n)$ is defined as

$$\mathcal{F}_0(n) = \int_0^{2\pi} d\varphi \, e^{in\varphi} \, \bar{V}(\varphi), \tag{D.16}$$

and n are $n = 0, \pm 1, \pm 2$.

D.2.2 Vector Mesons

For vector mesons the function $\mathcal{R}$ can be written as a linear combination of the terms

$$Z_1^{\alpha_1} Z_2^{\alpha_2} \qquad \text{and} \qquad k_i Z_1^{\alpha_1} Z_2^{\alpha_2},$$

where $\alpha_1, \alpha_2 = 0, \ldots, 3$. The first term is reduced to the non-vector case discussed in Subsect. D.2.1, because $Z_1^{\alpha_1} Z_2^{\alpha_2}$ can also be written as

$$c_0 + c_1 \exp[-i\lambda_3\varphi] + c_2 \exp[i\lambda_3\varphi]$$

with appropriated coefficients. The second term can be decomposed in three cases considered as follows:

Case 1 ($k_1 = \mathrm{k}\,\sin\theta\,\cos\varphi$): In this case we need to integrate factors like

$$(\mathrm{k}\sin\theta)\,\cos\varphi\, e^{in\varphi}\, \bar{V}(\varphi),$$

and the corresponding term of V, which we label V_1, is

$$V_1(\mathrm{p}', \theta', \mathrm{k}, \theta; \bar{\lambda}, W) = \delta_I \Lambda_m^4 g_m^2 f(\mathrm{p}', \mathrm{k})(\mathrm{k}\,\sin\theta)[c_0 \mathcal{F}_1(\bar{\lambda}) + c_1 \mathcal{F}_1(\bar{\lambda} - \lambda_3) + c_2 \mathcal{F}_1(\bar{\lambda} + \lambda_3)], \tag{D.17}$$

where

$$\mathcal{F}_1(n) = \int_0^{2\pi} d\varphi \, \cos\varphi \, e^{in\varphi} \, \bar{V}(\varphi), \tag{D.18}$$

with $n = 0, \pm 1, \pm 2$.

Case 2 ($k_2 = \mathrm{k} \sin\theta \sin\varphi$): We have also to consider terms like

$$(\mathrm{k} \sin\theta) \, \sin\varphi \, e^{in\varphi} \, \bar{V}(\varphi),$$

from which the following results for the corresponding V, which we label V_2,

$$V_2(\mathrm{p}', \theta', \mathrm{k}, \theta; \bar{\lambda}, W) = \delta_I \Lambda_m^4 g_m^2 f(\mathrm{p}', \mathrm{k})(\mathrm{k} \sin\theta)[c_0 \mathcal{F}_2(\bar{\lambda}) + c_1 \mathcal{F}_2(\bar{\lambda} - \lambda_3) + c_2 \mathcal{F}_2(\bar{\lambda} + \lambda_3)]. \tag{D.19}$$

The function $\mathcal{F}_2$ is defined as

$$\mathcal{F}_2(n) = \int_0^{2\pi} d\varphi \, \sin\varphi \, e^{in\varphi} \, \bar{V}(\varphi), \tag{D.20}$$

with $n = 0, \pm 1, \pm 2$.

Case 3 ($k_3 = \cos\theta$): No new φ-dependence appears. This case reduces to the non-vector meson case.

D.3 Functions $\mathcal{F}_l(n)$

The functions $\mathcal{F}_l(n)$ with $l = 0, 1, 2$ can be written in terms of the integrals

$$R_l = \int_0^{2\pi} \bar{V}(\varphi) \cos^l\varphi \, d\varphi,$$

for $l = 0, \ldots, 3$. The R_l integrals are performed analytically with the software program *Mathematica* and simplified afterward.

Appendix E. Momentum Transfer in the Two Terms of the Kernel

For the direct term the four-momentum transfer q is given by

$$q^2 = (p_1' - k_1)^2, \tag{E.1}$$

while for the exchange term it is given by

$$\hat{q}^2 = (p_1' - k_2)^2. \tag{E.2}$$

(See Fig. 2.)

When particle 1 has on-mass-shell positive energy one has

$$p_1' = (E_{\mathbf{p}'}, \mathbf{p}'), \tag{E.3}$$
$$p_2' = (W - E_{\mathbf{p}'}, -\mathbf{p}'), \tag{E.4}$$
$$k_1 = (E_{\mathbf{k}}, \mathbf{k}), \tag{E.5}$$
$$k_2 = (W - E_{\mathbf{k}}, -\mathbf{k}). \tag{E.6}$$

Then the momentum transfer reads

$$-q^2 = (\mathbf{p}' - \mathbf{k})^2 - (E_{\mathbf{p}'} - E_{\mathbf{k}})^2, \tag{E.7}$$
$$-\hat{q}^2 = (\mathbf{p}' + \mathbf{k})^2 - (E_{\mathbf{p}'} + E_{\mathbf{k}} - W)^2, \tag{E.8}$$

for the direct and exchange terms of the kernel, respectively.

As discussed in the text we propose an alternative expression for $\hat{q}^2$ (see Eq. (3.31)).

References

1. CLASS Collaboration: Niyazov, R. A., Weinstein, L. B., et al.: Phys. Rev. Lett. **91**, 252001 (2003)
2. Adam Jr., J., Gross, F., Jeschonnek, S., Ulmer, P., Van Orden, J. W.: Phys. Rev. **C66**, 044003 (2002)
3. Fachruddin, I., Elster, Ch., Glöckle, W.: Phys. Rev. **C62**, 044002 (2000); Nucl. Phys. **A689**, 507c (2001)
4. Fachruddin, I., Elster, Ch., Glöckle, W.: Phys. Rev. **C68**, 054003 (2003)
5. Gross, F.: Phys. Rev. **186**, 1448 (1969)
6. Gross, F., Van Orden, J. W., Holinde, K.: Phys. Rev. **C45**, 2094 (1992)
7. Elster, Ch., Thomas, J. H., Glöckle, W.: Few-Body Systems **24**, 55 (1998)
8. Elster, Ch., Schadow, W., Nogga, A., Glöckle, W.: Few-Body Systems **27**, 83 (1999); Schadow, W., Elster, Ch., Glöckle, W.: Few-Body Systems **28**, 15 (2000); Liu, H., Elster, Ch., Glöckle, W.: Few-Body Systems **33**, 241 (2003)
9. Ramalho, G., Arriaga, A., Peña, M. T.: Phys. Rev. **C65**, 034008 (2002)
10. Salpeter, E. E., Bethe, H. A.: Phys. Rev. **84**, 1232 (1951)
11. Gross, F.: Relativistic Quantum Mechanics and Field Theory, Chapt. 12. New York: Wiley 1993
12. Nieuwenhuis, T., Tjon, J. A.: Phys. Rev. Lett. **77**, 814 (1996)
13. Phillips, D. R., Wallace, S. J.: Phys. Rev. **C54**, 507 (1996)
14. Maung, K. M., Gross, F.: Phys. Rev. **C42**, 1681 (1990)
15. Ramalho, G., Arriaga, A., Peña, M. T.: Phys. Rev. **C60**, 047001 (1999)
16. Stadler, A., Gross, F.: Phys. Rev. Lett. **78**, 26 (1997)
17. Gross, F., Stadler, A., Van Orden, J. W., Devine, N.: Few-Body Systems Suppl. **8**, 269 (1995)
18. Caia, G. L., Pascalutsa, V., Wright, L. E.: Phys. Rev. **C69**, 034003 (2004)
19. Gersten, A., Solow, Z.: Phys. Rev. **D10**, 1031 (1974)
20. Gross, F., Riska, D. O.: Phys. Rev. **C36**, 1928 (1987)
21. Caia, G., Durso, J. W., Elster, Ch., Haidenbauer, J., Sibirtsev, A., Speth, J.: Phys. Rev. **C66**, 044006 (2002)
22. Ramalho, G.: PhD Thesis. Univ. Lisboa 2003 (unpublished)
23. Bystricky, J., Lehar, F., Winternitz, P.: J. Phys. (Paris) **39**, 1 (1978)
24. Brown, G. E., Jackson, A. D.: The Nucleon-Nucleon Interaction. Amsterdam: North-Holland 1976
25. Blankenbecler, R., Sugar, R.: Phys. Rev. **142**, 1051 (1966)
26. Mandelzweig, V. B., Wallace, S. J.: Phys. Lett. **B197**, 469 (1987); Wallace, S. J., Mandelzweig, V. B.: Nucl. Phys. **A503**, 673 (1989)
27. *NN*-Online: http://nn-online.org/NN/
28. Scanlon, J. P., et al.: Nucl. Phys. **41**, 401 (1963)
29. Kazarinov, Y. M., et al.: Sov. Phys. JETP **16**, 26 (1963)
30. Keeler, R. K., et al.: Nucl. Phys. **A377**, 529 (1982)
31. Lee, T. S. H., Riska, D. O.: Phys. Rev. Lett. **70**, 2237 (1993)
32. Hanhart, C., Miller, G. A., Myhrer, F., Sato, T., van Kolck, U.: Phys. Rev. **C63**, 044002 (2001)
33. Jacob, M., Wick, G. C.: Ann. Phys. (NY) **7**, 404 (1959)
34. Wick, G. C.: Ann. Phys. (NY) **18**, 65 (1962)
35. Carruthers, P. A.: Spin and Isospin in Particle Physics Theory, Chapt. 5. New York: Gordon and Breach 1971